Consecutive quasi-collisions in the planar circular RTBP

Joaquim FONT†, Ana NUNES‡and Carles SIMÓ†

†Departament de Matemàtica Aplicada i Anàlisi, Universitat de Barcelona, Gran Via 585, 08007 Barcelona, Spain

‡MAFUL/DFFCUL, Universidade de Lisboa, Av. Prof. Gama Pinto 2, 1649-003 Lisboa, Portugal

E-mail: `quim@maia.ub.es`,`anunes@lmc.fc.ul.pt`, `carles@maia.ub.es`

Abstract. In this paper we consider the planar circular restricted three body problem and, in particular, the existence of orbits which undergo consecutive close encounters with the small primary. The number of revolutions of the small bodies around the larger one between successive encounter can be chosen to be two arbitrary sequences of natural number, with constraints depending on the Jacobi constant. We prove that such orbits exist as a consequence of the fact that, when the mass parameter μ is small, the first return map defined on a region of phase space whose projection is a circle around the small primary is a 'horseshoe' map. The proof is constructive, in the sense that it is based on the computation of an approximate expression for this return map. When μ is small, the approximate return map contains the essential information about the dynamics from the quantitative as well as from the qualitative point of view. Using this information, we have been able to carry out a numerical study of this problem for μ up to 10^{-3}.

AMS classification scheme numbers: ————

Submitted to: *Nonlinearity*

1. Introduction

Consider the planar circular restricted three body problem, choosing, as usual, appropriate mass, length and time units so that the masses of the two primaries are $m_1 = 1-\mu$, $m_2 = \mu$, $\mu \in [0, 1/2)$, the angular velocity of their motion around the fixed center of mass is 1 and their positions in the plane are given in synodic coordinates (x, y) by $(\mu, 0)$ and $(\mu - 1, 0)$, respectively. In these coordinates, the equations of motion are (see, for instance [8])

$$\begin{aligned} \ddot{x} - 2\dot{y} &= \frac{\partial \Omega}{\partial x} = x - \frac{1-\mu}{r_1^3}(x-\mu) - \frac{\mu}{r_2^3}(x+1-\mu), \\ \ddot{y} + 2\dot{x} &= \frac{\partial \Omega}{\partial y} = y - \frac{1-\mu}{r_1^3} y - \frac{\mu}{r_2^3} y, \end{aligned} \tag{1}$$

where

$$\begin{aligned} \Omega &= \Omega(x, y) = \frac{1-\mu}{r_1} + \frac{\mu}{r_2} + \frac{1}{2}(x^2+y^2) + \frac{1}{2}\mu(1-\mu), \\ r_1^2 &= (x-\mu)^2 + y^2, \\ r_2^2 &= (x-\mu+1)^2 + y^2. \end{aligned}$$

Equations (1) have a first integral, the Jacobi function

$$\begin{aligned} C_J &= C_J(x, y, \dot{x}, \dot{y}) = 2\Omega(x, y) - (\dot{x}^2 + \dot{y}^2) \\ &= -\dot{x}^2 - \dot{y}^2 + 2\left(\frac{1-\mu}{r_1} + \frac{\mu}{r_2} + \frac{1}{2}(x^2+y^2) + \frac{1}{2}\mu(1-\mu)\right), \end{aligned} \tag{2}$$

and they are singular at the points $(x, y) = (\mu, 0)$ and $(x, y) = (\mu - 1, 0)$, which correspond to collision of the massless body Z with the big primary E and with the small primary M, respectively.

The purpose of this paper is to obtain an approximate expression for the return map defined on a suitable subset of a neighbourhood of the body M and to show the existence of solutions of equations (1) which go several times through this subset. More precisely, we shall say that a solution $\gamma(t)$, $t \in [t_1, t_2]$, of equations (1) is *$p - q$ resonant* , $p, q \in \mathbb{N}$ and relatively prime, $(p, q) = 1$, if both $\gamma(t_1)$ and $\gamma(t_2)$ are on a circle $\mathcal{C}$ of radius μ^α centered at M, with $\alpha \in (1/3, 1/2)$ a real parameter whose value will be specified later, if $\gamma(t)$ is outside the disk $\mathcal{D}$ of radius μ^α centered at M for all $t \in (t_1, t_2)$, and if moreover the time interval $t_2 - t_1$ between these successive approaches to M is such that

$$\frac{1}{2\pi}(t_1 - t_2) = q + \mathcal{O}(\mu^\alpha) = p\tau + \mathcal{O}(\mu^\alpha)$$

holds, where $2\pi\tau$ is the period of the orbit of Z as a two body problem with respect to E with the same initial conditions of γ at t_1. A solution of equations (1) will be called a *consecutive quasi-collision orbit* if it can be obtained by gluing together resonant orbits.

We shall prove that for any integer N the mass parameter can be chosen small enough so that any admissible (in a sense to be defined below) sequence (p_n, q_n), $n \in \mathbb{Z}$, $p_n, q_n < N$, $(p_n, q_n) = 1$, is realized by a solution of equations (1), that is, there exists a solution $\gamma(t)$ and a sequence of epochs $t_n, n \in \mathbb{Z}$ such that $\gamma([t_n, t_{n+1}])$ is a $p_n - q_n$ resonant orbit followed by a crossing of the disk $\mathcal{D}$.

The proof is made along the following steps:

(i) In Section 2 we derive an approximate expression for the *resonant strips*, that is, for the set of initial conditions on the circle $\mathcal{C}$ of radius μ^α around M which correspond to $p - q$ resonant orbits.

(ii) In Section 3 we obtain an approximate expression for the *OUT-map*, that is, the map that sends a point on a $p - q$ resonant strip to the position and velocity values of the orbit with those initial conditions at the time of its first intersection with the circle $\mathcal{C}$.

(iii) In Section 4 we obtain an approximate expression for the *IN-map*, that is, the map that sends the initial conditions of an orbit entering the disk $\mathcal{D}$ to the position and velocity values of that orbit at the time that it crosses again the circle $\mathcal{C}$ leaving the disk $\mathcal{D}$.

(iv) Finally, in Section 5 we match the errors made in the approximations involved in the computations of the OUT- and IN- maps and show that the composition of the OUT- and IN- maps defined on the resonant strips is a 'horseshoe' map.

In particular, our result implies the existence of infinitely many consecutive quasi-collision periodic orbits, corresponding to periodic sequences $(p_n, q_n)_{n\in\mathbb{Z}}$. These are what Poincaré called periodic orbits of the second species (POSS) ([7]). The existence of symmetric (with respect to the line joining the two primaries in synodic coordinates) POSS was proved by Perko ([6]), and by Henrard ([3]) and Marco and Niederman ([4]) by a different method. Most of the POSS that we find, however, are asymmetric. The existence of periodic orbits of the second species in a more general setting, which includes the RTBP, was proved by Bolotin and MacKay ([1]) through variational methods.

We remark that although we have considered the equations of motion for the circular RTBP, essentially the same steps can be carried out in the restricted elliptic case.

In Section 6 we present numerical computations of the resonant strips and of their images by the flow made for values of μ as high as 10^{-3} and make some concluding remarks on the interest of this result from the point of view of the design of spacecraft orbits.

2. The resonant strips

For the purpose of finding the resonant strips, as well as later for the purpose of computing the OUT-map, we shall approximate the solutions $\gamma(t)$ of equations (1) in the interval $[t_1, t_2]$ by orbits of the two body problem with respect to E with the same initial conditions of γ at t_1.

We shall start by bounding the error done in this approximation. Consider an orbit with initial conditions on the circle $\mathcal{C}$ of radius μ^α with

$$\frac{1}{3} < \alpha < \frac{1}{2} \tag{3}$$

so that the gravitational effect of the body M may be considered as a perturbation, and assume that the synodic velocity v_s at $t = t_1$

$$\begin{aligned} v_s^2 = & -C_J + 2\left(\frac{1-\mu}{r_1} + \frac{\mu}{\mu^\alpha} + \frac{x^2+y^2}{2} + \frac{1}{2}\mu(1-\mu)\right) \\ = & -C_J + 3 + 2\mu^{1-\alpha} + \mathcal{O}(\mu^{2\alpha}) \end{aligned} \tag{4}$$

is of order 1, that is, $C_J < 3$. Assume moreover that the orbit of Z as a two body problem with respect to E with the same initial conditions at $t = t_1$ is elliptic. Let $\mathbf{r}_2(t)$ be the position of Z with respect to M, so that $|\mathbf{r}_2(t)| = r_2(t)$. Then, $r_2(t_1) = \mu^\alpha$ and $\dot{r}_2(t_1) = v_s \cos a$, where a is the angle formed by the synodic velocity vector $\mathbf{v}_s(t_1)$ and $\mathbf{r}_2(t_1)$. Let us assume that $\cos a$ is positive and bounded away from zero, so that $\dot{r}_2(t_1) > k' > 0$; this means that we are considering an orbit leaving from the disk $\mathcal{D}$ at time t_1.

We want to obtain a lower bound for $r_2(t)$ as a function of t when $\mu^\alpha \le r_2 \le \mu^{\alpha/2}$. Since $\dot{r}_2(t) = \mathbf{v}_s(t)\cdot\mathbf{r}_2(t)/r_2(t)$, we have

$$\begin{aligned} \ddot{r}_2(t) &= \frac{\dot{\mathbf{v}}_s(t)\cdot\mathbf{r}_2(t)}{r_2(t)} + \mathbf{v}_s(t)\cdot\left(\frac{\dot{\mathbf{r}}_2(t)}{r_2(t)} - \frac{\mathbf{r}_2(t)\dot{r}_2(t)}{r_2^2(t)}\right) \\ &= \frac{\dot{\mathbf{v}}_s(t)\cdot\mathbf{r}_2(t)}{r_2(t)} + \left(\frac{v_s^2(t) - \dot{r}_2^2(t)}{r_2(t)}\right) \ge \frac{\dot{\mathbf{v}}_s(t)\cdot\mathbf{r}_2(t)}{r_2(t)}, \end{aligned}$$

where $\mathbf{a}\cdot\mathbf{b}$ means the scalar product of $\mathbf{a}$ and $\mathbf{b}$. From equations (1), we see that, close to M, the centrifugal and the gravitational terms due to E balance each other approximately, while the gravitational term due to M is bounded by $\mu^{1-2\alpha}$. More precisely, for $\mu^\alpha \le r_2 \le \mu^{\alpha/2}$ we have from equations (1) that $|\dot{\mathbf{v}}_s - 2\mathbf{v}_s \wedge \mathbf{e}_z| = \mathcal{O}(\mu^\beta)$, where $\mathbf{e}_z$ is a unit vector perpendicular to the plane of motion and $\beta = \min\{1-2\alpha, \alpha/2\}$. Therefore, for μ small enough, $\ddot{r}_2(t) \ge -3v_s$ or, using equations (4), $\ddot{r}_2(t) \ge -3\sqrt{3-C_J}$. Then, $\dot{r}_2(t) \ge \sqrt{3-C_J}(\cos a - 3(t-t_1))$ and $r_2(t) \ge \mu^\alpha + \sqrt{3-C_J}(\cos a(t-t_1) - 3(t-t_1)^2/2)$. This implies that $r_2(t)$ will become bigger than $\mu^{\alpha/2}$ after a time interval of order $\mu^{\alpha/2}$ and that, during that time interval, we have

$$r_2(t) \ge \mu^\alpha + b(t-t_1)$$

for some b bounded away from zero.

Consider equations (1) written as a first order system in the sidereal positions and velocities $\mathbf{q} \in \mathbb{R}^4$,

$$\dot{\mathbf{q}} = \mathbf{f}_{TB}(\mathbf{q}) + \Delta\mathbf{f}(\mathbf{q}, t), \tag{5}$$

where $\mathbf{f}_{TB}$ denotes the terms which correspond to the two body problem with respect to E, and let us show that the solution $\mathbf{q}(t)$ which corresponds to $\gamma(t)$ may be written in the form

$$\mathbf{q}(t) = \mathbf{q}_{TB}(t) + \mu^{1-\alpha}\Delta\mathbf{q}(t) + \mathcal{O}(\mu^{2-2\alpha}), \tag{6}$$

where $\mathbf{q}_{TB}(t)$ is the solution of the two body problem with respect to E with the same initial conditions at t_1 and $t \in (t_1, t_2)$. Since $\Delta\mathbf{f}$ is of order $\mu^{1-\alpha}$ whenever $r_2(t) \ge \mu^{\alpha/2}$,

(6) will hold for $t \in (t_1, t_2)$ provided that it holds when $\mu^\alpha \le r_2(t) \le \mu^{\alpha/2}$. Substituting (6) in (5) we obtain

$$\dot{\mathbf{q}}_{TB}(t) + \mu^{1-\alpha}\dot{\Delta\mathbf{q}}(t) + \mathcal{O}(\mu^{2-2\alpha}) = \mathbf{f}_{TB}(\mathbf{q}_{TB}(t)) + D\mathbf{f}_{TB}(\mathbf{q}_{TB}(t))\mu^{1-\alpha}\Delta\mathbf{q}(t) + \Delta\mathbf{f}(\mathbf{q}(t), t) + \mathcal{O}(\mu^{2-2\alpha}).$$

Therefore,

$$\dot{\Delta\mathbf{q}}(t) = D\mathbf{f}_{TB}(\mathbf{q}_{TB}(t))\Delta\mathbf{q}(t) + \frac{\Delta\mathbf{f}(\mathbf{q}(t), t)}{\mu^{1-\alpha}}$$

and, integrating,

$$\Delta\mathbf{q}(t) = \int_{t_1}^{t} \frac{\Delta\mathbf{f}(\mathbf{q}(s), s)}{\mu^{1-\alpha}} e^{\int_s^t D\mathbf{f}_{TB}(\mathbf{q}_{TB}(u))du} ds. \qquad (7)$$

Now

$$\Delta\mathbf{f}(\mathbf{q}(s), s) = \left(0, \mu\frac{q_1(s) - (\mu-1)\cos s}{r_2(s)^3}, 0, \mu\frac{q_2(s) - (\mu-1)\sin s}{r_2(s)^3}\right)$$

and hence

$$|\Delta\mathbf{f}(\mathbf{q}(s), s)| = \frac{\mu}{r_2(s)^2}.$$

On the other hand, since $\mathbf{q}_{TB}(t)$ is elliptic and $|t - s|$ is bounded (in fact, it is small), we have

$$|e^{\int_s^t D\mathbf{f}_{TB}(\mathbf{q}_{TB}(u))du}| \le M.$$

Introducing these bounds in (7) we obtain

$$\begin{aligned} |\Delta\mathbf{q}(t)| &\le \frac{M}{\mu^{1-\alpha}} \int_{t_1}^{t} |\Delta\mathbf{f}(\mathbf{q}(s), s)| ds = \frac{M}{\mu^{1-\alpha}} \int_{t_1}^{t} \frac{\mu}{r_2(s)^2} ds \\ &\le \frac{M}{\mu^{1-\alpha}} \int_{t_1}^{t} \frac{\mu}{(\mu^\alpha + b(s-t_1))^2} ds = \frac{M}{b}\left(1 - \frac{\mu^\alpha}{\mu^\alpha + k(t-t_1)}\right) \\ &\le \frac{M}{b}. \end{aligned}$$

Therefore, $|\Delta\mathbf{q}(t)|$ is bounded for t close to t_1. By the same argument, we have a similar bound for t close to t_2. If we assume that there are no close encounters between Z and M in the interval (t_1, t_2), then the error involved in the two-body problem approximation is of order $\mu^{1-\alpha}$ and we have the following

Lemma 2.1 *Let $\gamma(t)$, $t \in [t_1, t_2]$, be a resonant orbit and let a_i, $i = 1, 2$, be the angles formed by $\mathbf{v}_s(t_i)$ and $\mathbf{r}_2(t_i)$, $i = 1, 2$. Assume that $C_J < 3$, $|\cos a_i| > 0$, $i = 1, 2$, and that $\gamma(t)$ crosses the circle of radius $\mu^{\alpha/2}$ around M only twice. Then, $|\mathbf{q}(t) - \mathbf{q}_{TB}(t)| = \mathcal{O}(\mu^{1-\alpha})$ for $t \in [t_1, t_2]$, where $\mathbf{q}(t)$ is the orbit $\gamma(t)$ written in sidereal coordinates and $\mathbf{q}_{TB}(t)$ is the solution of the two body problem with respect to E with the same initial conditions as $\mathbf{q}(t)$.*

Let then

$$\frac{t_2 - t_1}{2\pi} = q + \tilde{\varepsilon} = p\tau + \tilde{\delta},$$

where $\tilde{\varepsilon} = \varepsilon'\mu^\alpha/2\pi + \mathcal{O}(\mu^{1-\alpha})$, $\tilde{\delta} = \delta'\mu^\alpha/2\pi + \mathcal{O}(\mu^{1-\alpha})$, $p, q \in \mathbb{N}$ for some parameters ε', δ' defined by these relations and assumed to be bounded. Denote now by $\mathbf{r}(t)$ the position of the body Z in sidereal coordinates, by $\mathbf{c}(t)$ the position of M also in sidereal coordinates. With this notation, the condition for resonance is

$$|\mathbf{r}(t_2) - \mathbf{c}(t_2)| = \mu^\alpha. \tag{8}$$

Using the fact that

$$\begin{aligned}
\mathbf{r}(t_1) &= (-1 + \mu + \mu^\alpha \cos\phi, \mu^\alpha \sin\phi),\\
\dot{\mathbf{r}}(t_1) &= (v\cos\psi, v\sin\psi),\\
\mathbf{c}(t_1) &= (-1 + \mu, 0),\\
\dot{\mathbf{c}}(t_1) &= (0, -1),\\
\mathbf{c}(t_2) &= \mathbf{c}(t_1) + \dot{\mathbf{c}}(t_1)\varepsilon'\mu^\alpha + \mathcal{O}(\mu^{1-\alpha}),\\
\mathbf{r}(t_2) &= \mathbf{r}(t_1 + \delta'\mu^\alpha) + \mathcal{O}(\mu^{1-\alpha})\\
&= \mathbf{r}(t_1) + \dot{\mathbf{r}}(t_1)\delta'\mu^\alpha + \mathcal{O}(\mu^{1-\alpha}),
\end{aligned}$$

where the first two equations define the coordinates ϕ, v and ψ, equation (8) implies, letting a side small terms $\mathcal{O}(\mu^{1-2\alpha})$,

$$\delta'^2 v^2 + 2\delta' v\cos(\psi - \phi) + \varepsilon'(\varepsilon' + 2\delta' v\sin\psi + 2\sin\phi) = 0. \tag{9}$$

Therefore, the periods τ for which the resonance condition is satisfied are those of the form

$$\tau = \frac{q}{p} + \frac{\tilde{\varepsilon} - \tilde{\delta}}{p},$$

where the coefficients of the terms of order μ^α in $\tilde{\varepsilon}$ and $\tilde{\delta}$ verify equation (9).

In order to determine the range of $k = \varepsilon' - \delta'$ along the ellipse given by (9) when $\cos\psi \neq 0$, we compute the values of k for which the lines $\varepsilon' - \delta' =$ *constant* are tangent to the ellipse and find two values k_1, k_2 given by

$$k_{1,2} = \frac{\cos\phi - v\sin(\phi - \psi) \pm \sqrt{1 + v^2 + 2v\sin\psi}}{v\cos\psi}.$$

We shall assume from now on that $\cos\psi \neq 0$. When $\cos\psi = 0$, equation (9) is that of two straight lines in the ϵ', δ' plane, and solutions can be found with $|\epsilon'|$, $|\delta'|$ and $|\epsilon' - \delta'|$ arbitrarily large. This happens because, when $\cos\psi = 0$, $\mathbf{r}(t_2) - \mathbf{r}(t_1)$ and $\mathbf{c}(t_2) - \mathbf{c}(t_1)$ are, up to terms of order μ^α, parallel. Hence, the resonance condition (8) does not, in this approximation, fix a range for ϵ' and δ'.

Therefore, the condition for resonance may be written as

$$\tau = \frac{q}{p} + \frac{k\mu^\alpha}{2\pi p} + \mathcal{O}(\mu^{1-\alpha}) \tag{10}$$

where $k_1 \leq k \leq k_2$. Using the following relations between the period τ and the energy E of the two-body orbit, and between the energy E and the sidereal velocity v,

$$\tau^{2/3} = \frac{(1-\mu)^{2/3}}{2|E|}, \qquad |E| = \frac{1-\mu}{\sqrt{1 + \mu^{2\alpha} - 2\mu^\alpha\cos\phi}} - \frac{v^2}{2},$$

the resonance condition (10) becomes, up to terms of order μ^α,

$$\left(\frac{q}{p}+\frac{k_1\mu^\alpha}{2\pi p}\right)^{2/3} \le \frac{(1-\mu)^{2/3}}{\frac{2(1-\mu)}{\sqrt{1+\mu^{2\alpha}-2\mu^\alpha\cos\phi}}-v^2} \le \left(\frac{q}{p}+\frac{k_2\mu^\alpha}{2\pi p}\right)^{2/3}. \tag{11}$$

Each of the terms of the last inequality may be expanded around $\mu=0$ up to terms of order μ^α. For the first and for the last term we get

$$\left(\frac{q}{p}+\frac{k_i\mu^\alpha}{2\pi p}\right)^{2/3} = \left(\frac{q}{p}\right)^{2/3}+\frac{2}{3}\left(\frac{p}{q}\right)^{1/3}\frac{k_i\mu^\alpha}{2\pi p}+\mathcal{O}(\mu^{2\alpha}),\quad i=1,2.$$

For the middle term we obtain, using the expansion $v=v_0+\Delta v\mu^\alpha+\mathcal{O}(\mu^{2\alpha})$ for the sidereal velocity,

$$\frac{(1-\mu)^{2/3}}{\frac{2(1-\mu)}{\sqrt{1+\mu^{2\alpha}-2\mu^\alpha\cos\phi}}-v^2} = \frac{1}{2-v_0^2}+\mu^\alpha\left(\frac{2v_0\Delta v-2\cos\phi}{(2-v_0^2)^2}\right)+\mathcal{O}(\mu^{2\alpha}).$$

Equating the terms of order zero in μ^α we have

$$\frac{1}{2-v_0^2} = \left(\frac{q}{p}\right)^{2/3},$$

that is, v_0 is determined by the integers p and q by

$$v_0=\sqrt{2-\left(\frac{p}{q}\right)^{2/3}}$$

and p and q are subject to the restriction $p/q<2\sqrt{2}$. Taking into account the terms of order μ^α inequality (11) implies

$$|\Delta v-B|\le C \tag{12}$$

where

$$B(\phi,\psi,q,p)=\frac{\cos\phi}{v_0}+\frac{1}{3p}(2-v_o^2)^{5/2}\frac{\cos\phi-v_0\sin(\phi-\psi)}{2\pi v_0^2\cos\psi},$$
$$C(\phi,\psi,q,p)=\frac{1}{3p}(2-v_0^2)^{5/2}\frac{\sqrt{1+v_0^2+2v_0\sin\psi}}{2\pi v_0^2|\cos\psi|}.$$

Therefore, the resonant sidereal velocity must verify

$$v=\sqrt{2-\left(\frac{p}{q}\right)^{2/3}}+\Delta v\mu^\alpha+\mathcal{O}(\mu^{1-\alpha}), \tag{13}$$

where $\Delta v(\phi,\psi,q,p)$ obeys the inequality (12).

We are interested however in an expression for the resonant velocities in terms of coordinates on the circle $\mathcal{C}$ of radius μ^α associated to the moving reference frame where both primaries are fixed, that is, in terms of synodic coordinates. Let us then characterize the initial conditions of the particle as it leaves the circle by the triad

ϕ, v_s, ψ_s, where ϕ is the angular coordinate on the circle defined above, v_s is the modulus and ψ_s the direction of the velocity of the particle in synodic coordinates. Since we have

$$\begin{aligned} v\cos\psi &= v_s\cos\psi_s - \mu^\alpha\sin\phi, \\ v\sin\psi &= -1+\mu+v_s\sin\psi_s+\mu^\alpha\cos\phi, \end{aligned} \tag{14}$$

the two sets of coordinates on $\mathcal{C}$, (ϕ, v_s, ψ_s) and (ϕ, v, ψ) are related by the equations

$$\begin{aligned} v &= \sqrt{1+v_s^2-2v_s\sin\psi_s-2\mu^\alpha(v_s\sin(\phi-\psi_s)+\cos\phi)}, \\ \psi &= \psi_s - \arcsin\left(\frac{\cos\psi_s-\mu^\alpha\cos(\psi_s-\phi)}{v}\right), \end{aligned} \tag{15}$$

the coordinate ϕ being the same either in sidereal or in synodic coordinates.

Squaring the first equation in (15) and introducing in (13) we obtain, using (14), the following approximate expression for the resonant synodic velocity $v_s^R(\phi,\psi_s,p,q)$, that is, the value of the modulus of the synodic velocity on the circle $\mathcal{C}$ which, for each admissible value of (ϕ,ψ_s,p,q), gives rise to a $p-q$ resonant orbit:

$$\begin{aligned} v_s^R(\phi,\psi_s,p,q) = v_s^0(\phi,\psi_s,p,q) + \mu^\alpha B_s(\phi,\psi_s,p,q) \\ + \xi\mu^\alpha C_s(\phi,\psi_s,p,q) + \mathcal{O}(\mu^{1-\alpha}), \end{aligned} \tag{16}$$

where $\xi \in (-1,1)$,

$$\begin{aligned} v_s^0(\phi,\psi_s,p,q) &= \sin\psi_s \pm \sqrt{v_0^2-\cos^2\psi_s}, \\ B_s(\phi,\psi_s,p,q) &= \frac{1}{\pm\sqrt{v_0^2-\cos^2\psi_s}}\left(2\cos\phi + \left(v_s^0 - \frac{e}{\cos\psi_s}\right)\sin(\phi-\psi_s)\right), \\ C_s(\phi,\psi_s,p,q) &= \frac{e}{\pm\sqrt{v_0^2-\cos^2\psi_s}\cos\psi_s}, \end{aligned}$$

and

$$v_0^2 = 2 - \left(\frac{p}{q}\right)^{2/3}, \qquad e = \frac{(2-v_0^2)^{5/2}}{6\pi p}.$$

Note 2.1 *In the above expression for v_s^0 there can be two solutions for some values of p, q and ψ_s, but the sign must always be chosen so that $v_s^0 > 0$.*

Note 2.2 *The restriction $\cos\psi$ bounded away from 0 now implies that (16) holds whenever $\cos\psi_s$ is bounded away from 0.*

We must now take into account the fact that the exact problem possesses the Jacobi constant (2) as a first integral. Using (16) in (4) we get

$$(v_s^R)^2 = 3 - C_J + \mathcal{O}(\mu^{1-\alpha}).$$

Equating the terms of order zero in μ^α we obtain

$$(v_s^0)^2 = 3 - C_J,$$

and therefore

$$\sin\psi_s \pm \sqrt{v_0^2-\cos^2\psi_s} = \sqrt{3-C_J}, \tag{17}$$

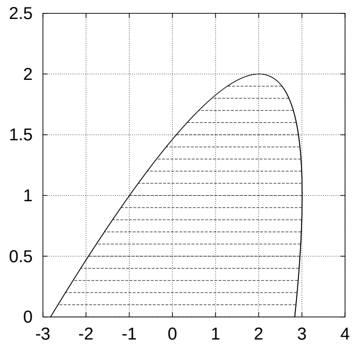

Figure 1. Plotting C_J on the horizontal axis and $(p/q)^{2/3}$ on the vertical axis, the dashed region is the admissible region given by inequality (19).

which solves the ambiguity in the sign of the square root. Denoting by $\tilde{\psi}_s$ the solution of equation (17) for given p, q and C_J, the following relations hold

$$\begin{aligned} \sin\tilde{\psi}_s &= \frac{4 - C_J - v_0^2}{2\sqrt{3 - C_J}}, \\ \cos\tilde{\psi}_s &= \sigma\frac{\sqrt{4v_0^2 - (2 - C_J - v_0^2)^2}}{2\sqrt{3 - C_J}}, \end{aligned} \tag{18}$$

where $\sigma = \pm 1$ is the sign of $\cos\tilde{\psi}_s$ and is determined, for given ϕ, by the fact that (ϕ, ψ_s, v_s) are initial conditions of orbits *leaving* the disk $\mathcal{D}$. Clearly, equations (18) imply the inequality

$$-2\sqrt{3 - C_J} \leq 2 - C_J + \left(\frac{p}{q}\right)^{2/3} \leq 2\sqrt{3 - C_J}, \tag{19}$$

which represents, given C_J, a restriction on the possible values of p, q.

Comparing (19) with the condition $p/q < 2\sqrt{2}$ found before, we see that (19) is more restrictive and hence it is enough to take (19) into account. If (19) is verified with strict inequalities, then the condition $\cos\psi_s$ bounded away from 0 is automatically satisfied. Given C_J, we shall say that a pair (p, q) is *admissible* if (19) is verified strictly (see Figure 1). Note that this excludes the orbits which are close to orbits of the two body problem with perpendicular crossings of the x-axis.

Taking $\psi_s = \tilde{\psi}_s + \mu^\alpha\Delta\psi_s + \mathcal{O}(\mu^{1-\alpha})$, $\phi \in S^1$, v determined in terms of $\xi \in (-1, 1)$ by the resonant condition (16), the additional constraint imposed by the Jacobi constant is verified up to terms of μ^α if

$$\mathcal{K}(p, q, C_J)\Delta\psi_s + B_s(\phi, \tilde{\psi}_s, p, q) + \xi C_s(\phi, \tilde{\psi}_s, p, q) = 0,$$

where

$$\mathcal{K}(p, q, C_J) = \frac{2(3 - C_J)\cos\tilde{\psi}_s}{2 - C_J + v_0^2} = \sigma\frac{\sqrt{3 - C_J}\sqrt{4v_0^2 - (2 - C_J - v_0^2)^2}}{2 - C_J + v_0^2},$$

different from zero if (p, q) is admissible. We shall call $p - q$ *resonant strip* the two dimensional subset of the space of the synodic coordinates and velocities which corresponds, for given C_J, to initial conditions *leaving* the disk $\mathcal{D}$ of $p-q$ resonant solutions. Therefore, we may take as coordinates on the $p-q$ resonant strips either $(\phi, \Delta\psi_s)$ or (ϕ, ξ). The latter will be our choice from now on.

3. The OUT-map

The OUT-map, that is, the map that sends a point on a $p-q$ resonant strip to the position and velocity values of the orbit with those initial conditions at the time of its first intersection with the circle $\mathcal{C}$, is easy to compute in sidereal coordinates. Recall that the time t_2-t_1 between two consecutive intersections with the circle $\mathcal{C}$ is of the form $t_2-t_1 = 2\pi q + \varepsilon'\mu^\alpha + \mathcal{O}(\mu^{1-\alpha}) = 2\pi p\tau + \delta'\mu^\alpha + \mathcal{O}(\mu^{1-\alpha})$ for a given $p-q$ resonant strip, and $2\pi\tau$ is the period of the two-body problem orbit with respect to E with the same initial conditions. Then, denoting again by (ϕ, ψ, v) the set of coordinates at time t_1 associated to the sidereal reference frame, the position and sidereal velocity $(\mathbf{r}(t_2), \mathbf{v}(t_2))$ at time t_2 when the orbit enters in the disk $\mathcal{D}$ are given by

$$\begin{aligned}
\mathbf{r}(t_2) &= \mathbf{r}(t_1 + 2\pi p\tau + \delta'\mu^\alpha + \mathcal{O}(\mu^{1-\alpha})) = \mathbf{r}(t_1) + \mathbf{v}(t_1)\delta'\mu^\alpha + \mathcal{O}(\mu^{1-\alpha}) \\
&= (-1+\mu+\mu^\alpha\cos\phi, \mu^\alpha\sin\phi) + \delta'\mu^\alpha(v\cos\psi, v\sin\psi) + \mathcal{O}(\mu^{1-\alpha}), \qquad (20) \\
\mathbf{v}(t_2) &= \mathbf{v}(t_1) + \delta'\mu^\alpha(1,0) + \mathcal{O}(\mu^{1-\alpha}) \\
&= (v\cos\psi + \delta'\mu^\alpha, v\sin\psi) + \mathcal{O}(\mu^{1-\alpha}), \qquad (21)
\end{aligned}$$

with ε' and δ' satisfying equation (9).

We shall use equations (20) and (21) to obtain an approximate expression for (ϕ_e, ψ_e, v_e) associated to the synodic coordinates at time t_2 in terms of the coordinates (ϕ_s, ψ_s, v_s) of a point on a given resonant strip. Since the position angle ϕ on the circle $\mathcal{C}$ is the same in the sidereal and in the synodic reference frame, from (20) and (8) we obtain, equating the terms of order μ^α,

$$\begin{aligned}
\sin\phi_e &= \sin\phi + \delta' v\sin\psi + \varepsilon' + \mathcal{O}(\mu^{1-2\alpha}), \\
\cos\phi_e &= \cos\phi + \delta' v\cos\psi + \mathcal{O}(\mu^{1-2\alpha}),
\end{aligned} \qquad (22)$$

because the position of the body M at time t_2 in the sidereal reference frame is $\mathbf{r}_M(t_2) = (-1+\mu, -\varepsilon'\mu^\alpha) + \mathcal{O}(\mu^{1-\alpha})$. In order to obtain the equations of the map for the remaining variables we shall start by writing (21) in terms of synodic coordinates via the transformation

$$\begin{pmatrix} \dot{x} \\ \dot{y} \end{pmatrix}_{syn} = \begin{pmatrix} 1 & \varepsilon'\mu^\alpha \\ -\varepsilon'\mu^\alpha & 1 \end{pmatrix} \begin{pmatrix} \dot{x} \\ \dot{y} \end{pmatrix}_{sid} + \begin{pmatrix} -\varepsilon'\mu^\alpha & 1 \\ -1 & -\varepsilon'\mu^\alpha \end{pmatrix} \begin{pmatrix} x \\ y \end{pmatrix}_{sid},$$

which holds at time t_2 up to terms of order $\mu^{1-\alpha}$. Introducing (21), we obtain

$$\begin{pmatrix} v_e\cos\psi_e \\ v_e\sin\psi_e \end{pmatrix} = \begin{pmatrix} v\cos\psi + \mu^\alpha(\delta' + \varepsilon'(v\sin\psi+1) + \sin\phi + \delta' v\sin\psi) \\ 1 + v\sin\psi - \mu^\alpha(\cos\phi + \varepsilon' v\cos\psi + \delta' v\cos\psi) \end{pmatrix} + \mathcal{O}(\mu^{1-\alpha}). \qquad (23)$$

Substituting (14) in (23) we get

$$\begin{aligned}
v_e\cos\psi_e &= v_s\cos\psi_s + \mu^\alpha\left(v_s\sin\psi_s(\delta'+\varepsilon')\right) + \mathcal{O}(\mu^{1-\alpha}), \\
v_e\sin\psi_e &= v_s\sin\psi_s - \mu^\alpha\left(v_s\cos\psi_s(\delta'+\varepsilon')\right) + \mathcal{O}(\mu^{1-\alpha}),
\end{aligned} \qquad (24)$$

and substituting (14) in (22) we obtain

$$\begin{array}{rcl}\sin\phi_e &=& \sin\phi_s + \delta'(v_s\sin\psi_s - 1) + \varepsilon' + \mathcal{O}(\mu^{1-2\alpha}),\\ \cos\phi_e &=& \cos\phi_s + \delta' v_s\cos\psi_s + \mathcal{O}(\mu^{1-2\alpha}).\end{array} \tag{25}$$

Squaring and adding the two equations (24) we obtain the OUT-map equation for the synodic velocity

$$v_e = v_s + \mathcal{O}(\mu^{1-\alpha}).$$

We must still derive from (24) and (25) the explicit equations of the OUT-map for the angular coordinates in terms of the coordinates (ϕ,ξ) on a given $p-q$ resonant strip. Since, from (9)

$$\begin{array}{rcl}\varepsilon'-\delta' &=& -\dfrac{\sin(\phi-\psi_s)}{\cos\psi_s} + \dfrac{\xi}{\cos\psi_s},\\ \delta' &=& -\dfrac{\cos\phi}{v_s\cos\psi_s} - \dfrac{\sin\psi_s}{v_s\cos\psi_s}\xi \pm \dfrac{\sqrt{1-\xi^2}}{v_s},\\ \varepsilon' &=& -\dfrac{\cos\phi + v_s\sin(\phi-\psi_s)}{v_s\cos\psi_s} + \dfrac{v_s-\sin\psi_s}{v_s\cos\psi_s}\xi \pm \dfrac{\sqrt{1-\xi^2}}{v_s},\\ \varepsilon'+\delta' &=& -\dfrac{2\cos\phi + v_s\sin(\phi-\psi_s)}{v_s\cos\psi_s} + \dfrac{v_s-2\sin\psi_s}{v_s\cos\psi_s}\xi \pm 2\dfrac{\sqrt{1-\xi^2}}{v_s},\end{array} \tag{26}$$

equations (25) become

$$\begin{array}{rcl}\cos\phi_e &=& -\sin\psi_s\xi \pm \sqrt{1-\xi^2}\cos\psi_s + \mathcal{O}(\mu^{1-2\alpha}),\\ \sin\phi_e &=& \cos\psi_s\xi \pm \sqrt{1-\xi^2}\sin\psi_s + \mathcal{O}(\mu^{1-2\alpha}).\end{array} \tag{27}$$

The square root in equations (26) and (27) is affected by the sign $\pm$. In fact, for fixed C_J, p and q, there would be in general two solutions given ψ_s, ϕ_s. Clearly, the solution associated to the first intersection with the circle $\mathcal{C}$ corresponds to the choice of the $-$ sign, because we must have $\cos(\psi_e-\phi_e)<0$ and $\cos(\phi_e-\psi_e)<0 \iff \pm\sqrt{1-\xi^2}<0$. Taking this into account, the equation for ϕ_e may also be written in the form $\phi_e = \psi_s + \pi - \arcsin\xi + \mathcal{O}(\mu^{1-2\alpha})$. Summing up, the approximate expression for the OUT-map on a $p-q$ resonant strip is

$$\begin{array}{l}\phi_e = \psi_s + \pi - \arcsin\xi + \mathcal{O}(\mu^{1-2\alpha}),\\ \psi_e = \psi_s - (\varepsilon'+\delta')\mu^{\alpha} + \mathcal{O}(\mu^{1-\alpha}),\\ v_e = v_s + \mathcal{O}(\mu^{1-\alpha}),\end{array} \tag{28}$$

where $\varepsilon'+\delta'$ is given by equations (26) with the $-$ choice of sign. Using the Jacobi integral (2) we may write, instead of the third equation (28), the more accurate expression

$$v_e = \sqrt{3-C_J-3\mu} + \frac{2\mu^{1-\alpha} + 3\cos^2\phi_e\mu^{2\alpha}}{2\sqrt{3-C_J}} + \mathcal{O}(\mu^{3\alpha}) \tag{29}$$

4. The IN-map

In this section we shall derive an approximate expression for the IN-map that sends initial conditions (ϕ_e,ψ_e,v_e) associated to synodic coordinates which correspond to orbits *entering* the disk $\mathcal{D}$ to the values (ϕ_s, ψ_s, v_s) corresponding to the first intersection of these orbits with the boundary circle $\mathcal{C}$.

Since we are dealing now with orbits that approach one of the system's singularities, collision with the small primary M, we shall have to choose appropriate coordinates to regularize it. This can be achieved for instance with the Levi-Civita transformation, but we want to take into account as well the fact that the motion takes place $\mu^\alpha-$close to the body M, and hence we shall combine the use of Levi-Civita variables with a convenient rescaling, similar to the one that is used to obtain Hill's equations for the motion of the moon (see for instance [8]).

Let

$$\begin{aligned} a_1 &= \mu^{-1/3}(x+1-\mu), \\ a_2 &= \mu^{-1/3}y, \\ b_1 &= \mu^{-1/3}\dot{x} - a_2, \\ b_2 &= \mu^{-1/3}\dot{y} + a_1, \end{aligned} \tag{30}$$

where x, y, $\dot{x}$ and $\dot{y}$ are the synodic coordinates and velocities. The equations of motion and the Jacobi constant become

$$\begin{aligned} \dot{a}_1 &= b_1 + a_2, \\ \dot{a}_2 &= b_2 - a_1, \\ \dot{b}_1 &= b_2 + 2a_1 - \frac{a_1}{|\mathbf{a}|^3} + \mu^{1/3}\left(3a_1^2 - 3a_2^2/2\right) + \mathcal{O}(\mu^{2/3}), \\ \dot{b}_2 &= -b_1 - a_2 - \frac{a_2}{|\mathbf{a}|^3} - \mu^{1/3}\left(3a_1a_2\right) + \mathcal{O}(\mu^{2/3}), \end{aligned} \tag{31}$$

$$\begin{aligned} \tilde{C} &= \mu^{-2/3}(3 - C_J - 3\mu) \\ &= |\mathbf{b}|^2 - 2a_1^2 + a_2^2 - 2(a_1b_2 - a_2b_1) - \frac{2}{|\mathbf{a}|} - \mu^{1/3}(2a_1^3 - 3a_1a_2^2) + \mathcal{O}(\mu^{2/3}). \end{aligned} \tag{32}$$

We shall now introduce the time dependent change of variables

$$\begin{aligned} \tilde{a}_1 &= a_1\cos t - a_2\sin t, \\ \tilde{a}_2 &= a_1\sin t + a_2\cos t, \\ \tilde{b}_1 &= b_1\cos t - b_2\sin t, \\ \tilde{b}_2 &= b_1\sin t + b_2\cos t. \end{aligned} \tag{33}$$

Equations (31) and (32) become now

$$\begin{aligned} \dot{\tilde{a}}_1 &= \tilde{b}_1, \\ \dot{\tilde{a}}_2 &= \tilde{b}_2, \\ \dot{\tilde{b}}_1 &= -\frac{\tilde{a}_1}{|\tilde{\mathbf{a}}|^3} + \tilde{a}_1(2\cos^2 t - \sin^2 t) + 3\tilde{a}_2\sin t\cos t + \mathcal{O}(\tilde{\mathbf{a}}^2, \mu^{1/3}) + \mathcal{O}(\mu^{2/3}), \\ \dot{\tilde{b}}_2 &= -\frac{\tilde{a}_2}{|\tilde{\mathbf{a}}|^3} + 3\tilde{a}_1\sin t\cos t + \tilde{a}_2(2\sin^2 t - \cos^2 t) + \mathcal{O}(\tilde{\mathbf{a}}^2, \mu^{1/3}) + \mathcal{O}(\mu^{2/3}), \end{aligned} \tag{34}$$

$$\tilde{C} = |\tilde{\mathbf{b}}|^2 - \frac{2}{|\tilde{\mathbf{a}}|} - 2(\tilde{a}_1\tilde{b}_2 - \tilde{a}_2\tilde{b}_1) + \mathcal{O}(\tilde{\mathbf{a}}^2) + \mathcal{O}(|\tilde{\mathbf{a}}|^3, \mu^{1/3}) + \mathcal{O}(\mu^{2/3}). \tag{35}$$

Introducing in (34) and (35) the Levi-Civita regularization

$$\tilde{a}_1 + i\tilde{a}_2 = \tilde{z}^2, \quad \tilde{b}_1 + i\tilde{b}_2 = \frac{\tilde{w}}{\bar{\tilde{z}}}, \quad , \frac{dt}{d\rho} = 2|\tilde{z}|^2, \tag{36}$$

we obtain

$$
\begin{aligned}
\tilde{z}' &= \tilde{w}, \\
\tilde{w}' &= \frac{|\tilde{w}|^2}{\bar{\tilde{z}}} - \frac{2\tilde{z}}{|\tilde{z}|^2} + \mathcal{O}(\tilde{z}^5) + \mathcal{O}(\mu^{2/3}),
\end{aligned} \tag{37}
$$

$$
\tilde{C} = \frac{|\tilde{w}|^2}{|\tilde{z}|^2} - \frac{2}{|\tilde{z}|^2} + i(\tilde{w}\bar{\tilde{z}} - \tilde{z}\bar{\tilde{w}}) + \mathcal{O}(\tilde{z}^4) + \mathcal{O}(\mu^{2/3}), \tag{38}
$$

where ' denotes the derivative with respect to ρ. Using (38) we may write instead of (37)

$$
\begin{aligned}
\tilde{z}' &= \tilde{w}, \\
\tilde{w}' &= \tilde{C}\tilde{z} - i\tilde{z}(\tilde{w}\bar{\tilde{z}} - \tilde{z}\bar{\tilde{w}}) + \mathcal{O}(\tilde{z}^5) + \mathcal{O}(\tilde{z}^7, \mu^{1/3}) + \mathcal{O}(\mu^{2/3}).
\end{aligned}
$$

The scaling

$$
\sqrt{\epsilon} z = \tilde{z}, \quad \sqrt{\epsilon} w = \frac{\tilde{w}}{\sqrt{\tilde{C}}}, \tag{39}
$$

with $\epsilon = \mu^{\alpha - 1/3}$ maps the disk of radius μ^α around $(-1+\mu, 0)$ in synodic coordinates on the unit ball in the complex z plane. In the (z, w) variables and changing time according to $s = \sqrt{\tilde{C}}\rho$, the equations of motion and the Jacobi integral become

$$
\begin{aligned}
\dot{z} &= w, \\
\dot{w} &= z - i\frac{\epsilon}{\sqrt{\tilde{C}}} z(w\bar{z} - z\bar{w}) + \mathcal{O}(\frac{\epsilon^2}{\tilde{C}}),
\end{aligned} \tag{40}
$$

where the dot now denotes the derivative with respect to s, and

$$
\frac{2}{\epsilon\tilde{C}} = |w|^2 - |z|^2 + i\frac{\epsilon}{\sqrt{\tilde{C}}}|z|^2(w\bar{z} - z\bar{w}) + \mathcal{O}(\mu^{2\alpha}). \tag{41}
$$

Notice that (41) implies that when $|z| \leq 1$, $|z|$ and $|w|$ are of the same order. Notice also that $w\bar{z} - z\bar{w}$ is a constant for the order zero equations (40). Then, we may write the equations of motion in the form

$$
\begin{aligned}
\dot{z} &= w, \\
\dot{w} &= \mathcal{L}z + \mathcal{O}(\mu^{2\alpha}),
\end{aligned} \tag{42}
$$

where $\mathcal{L} = 1 - i\epsilon(w(0)\bar{z}(0) - z(0)\bar{w}(0))/\sqrt{\tilde{C}}$. In order to bound the error associated to the truncated equations (42) we must determine the order of magnitude of the crossing time of the unit ball. Since the approximate solution is of the form $z_0(s) = z(0)\cosh\sqrt{\mathcal{L}}s + (w(0)/\sqrt{\mathcal{L}})\sinh\sqrt{\mathcal{L}}s$, we have that the condition $|z_0| = 1$ is fulfilled for $s = 0$ and for s_0 such that

$$
e^{2\sqrt{\mathcal{L}}s_0} = \frac{1 + \frac{|w(0)|^2}{\mathcal{L}} - \frac{1}{\sqrt{\mathcal{L}}}(w(0)\bar{z}(0) + z(0)\bar{w}(0))}{1 + \frac{|w(0)|^2}{\mathcal{L}} + \frac{1}{\sqrt{\mathcal{L}}}(w(0)\bar{z}(0) + z(0)\bar{w}(0))} \tag{43}
$$

and the error Δz, Δw is of order

$$
\Delta z = \frac{\cosh\sqrt{\mathcal{L}}s_0 - 1}{\mathcal{L}}\mathcal{O}(\mu^{2\alpha}), \Delta w = \frac{\sinh\sqrt{\mathcal{L}}s_0}{\sqrt{\mathcal{L}}}\mathcal{O}(\mu^{2\alpha}).
$$

Now, in terms of the synodic coordinates (ϕ, v, ψ) at $s = 0$, that is, on the circle $\mathcal{C}$ and going into the disk $\mathcal{D}$, we have

$$\mathcal{L} = 1 + \frac{2\mu^\alpha}{3 - C_J - 3\mu}(\mu^\alpha + v\sin(\psi - \phi)),$$

$$w(0)\bar{z}(0) + z(0)\bar{w}(0) = \frac{2v\cos(\psi - \phi)}{\sqrt{3 - C_J - 3\mu}},$$

$$|w(0)|^2 = \frac{v^2}{3 - C_J - 3\mu} - 2\mu^\alpha \frac{v\sin(\psi - \phi)}{3 - C_J - 3\mu} + \frac{\mu^{2\alpha}}{3 - C_J - 3\mu}.$$

Substituting into (43) and using (29) we find that, close to collision, that is, when $|\psi - \phi|$ close to π,

$$e^{2\sqrt{\mathcal{L}}s_0} = \mathcal{O}(\mu^{-2\alpha})$$

so that

$$\Delta z = \mathcal{O}(\mu^\beta), \quad \Delta w = \mathcal{O}(\mu^\beta)$$

with $\beta = 2\alpha$ (resp. $\beta = \alpha$) for orbits away from (resp. close to) collision. Going back to synodic coordinates involves in equation (33) the synodic crossing time T of the disk $\mathcal{D}$. From (36) and (39), we have

$$T = \frac{2\mu^\alpha}{\sqrt{3 - C_J - 3\mu}} \int_0^{s_*} |z(s)|^2 \, ds,$$

where $z(s)$ is the solution and s_* the crossing time of the unit ball for the full equations (42). Since $|z(s) - z_0(s)| = \mathcal{O}(\mu^\beta)$, $|s_* - s_0| = \mathcal{O}(\mu^\beta)$ and $s_0 = \mathcal{O}(\log\mu)$,

$$\begin{aligned} T &= \frac{2\mu^\alpha}{\sqrt{3 - C_J}} \int_0^{s_0} |z_0(s)|^2 \, ds + \mathcal{O}(\mu^{\beta+\alpha}\log\mu) \\ &= T_0 + \mathcal{O}(\mu^{\beta+\alpha}\log\mu) \end{aligned}$$

where

$$T_0 = -\frac{2\mu^\alpha}{\sqrt{3 - C_J}}\cos(\psi - \phi).$$

From (42) and (43) the explicit expression for the approximate IN-map $(z_s(z(0), w(0)), w_s(z(0), w(0))$ is

$$\begin{pmatrix} z_s \\ w_s \end{pmatrix} = \frac{1}{\mathcal{R}} \begin{pmatrix} \mathcal{L} + R^2 & -2R\cos(b - a) \\ -2\mathcal{L}R\cos(b - a) & \mathcal{L} + R^2 \end{pmatrix} \begin{pmatrix} z(0) \\ w(0) \end{pmatrix} + \mathcal{O}(\mu^\beta), \quad (44)$$

where a, b and R are defined by means of $z(0) = e^{ia}$, $w(0) = Re^{ib}$. Hence $\mathcal{L} = 1 + \dfrac{2\mu^\alpha R\sin(b - a)}{\sqrt{3 - C_J - 3\mu}}$ and $\mathcal{R} = \sqrt{(\mathcal{L} - R^2)^2 + 4R^2\mathcal{L}\sin^2(b - a)}$.

As a, b and R are given, in terms of the synodic coordinates (ϕ, v, ψ) by

$$a = \phi/2, \quad , b = \psi - \frac{\phi}{2} + \mu^\alpha \frac{\cos(\psi - \phi)}{v} + \mathcal{O}(\mu^{2\alpha}),$$

$$R = \sqrt{\frac{v^2 + 2\mu^\alpha v\sin(\psi - \phi)}{3 - C_J}} + \mathcal{O}(\mu^{2\alpha}),$$

we obtain for the IN-map far from collision, that is, when $\sin(\psi_e - \phi_e)$ is bounded away from zero and big compared with μ^α,

$$\begin{aligned}
z_s &= \frac{e^{i\phi_e/2} - \cos(\psi_e-\phi_e)e^{i(\psi_e-\phi_e/2)}}{|\sin(\psi_e-\phi_e)|} \\
&\quad +\mu^\alpha\left(\frac{\sin(\psi_e-\phi_e)e^{i\phi_e/2} + i\sin^2(\psi_e-\phi_e)e^{i(\psi_e-\phi_e/2)}}{|\sin(\psi_e-\phi_e)|\sqrt{3-C_J}}\right) \\
&\quad -\frac{\cos(\psi_e-\phi_e)e^{i(\psi-\phi/2)}}{(3-C_J)|\sin(\psi_e-\phi_e)|}\mu^{1-\alpha} + \mathcal{O}(\mu^{2\alpha}), \\
w_s &= \frac{e^{i(\psi_e-\phi_e/2)} - \cos(\psi_e-\phi_e)e^{i\phi_e/2}}{|\sin(\psi_e-\phi_e)|} + \mu^\alpha\left(\frac{i\sin^2(\psi_e-\phi_e)e^{i\phi_e/2}}{|\sin(\psi_e-\phi_e)|\sqrt{3-C_J}}\right) \\
&\quad +\frac{e^{i(\psi-\phi/2)}}{(3-C_J)|\sin(\psi_e-\phi_e)|}\mu^{1-\alpha} + \mathcal{O}(\mu^{2\alpha}),
\end{aligned}$$

where we have used (29).

Going back from z_s, w_s to synodic coordinates through the changes of variables (39), (36), (33) and (30), we obtain, away from collision,

$$\begin{aligned}
\phi_s &= 2\psi_e - \phi_e + \pi + 4\mu^\alpha\frac{\cos(\psi_e-\phi_e)}{\sqrt{3-C_J}} \\
&\quad -\frac{2\cos(\psi_e-\phi_e)}{(3-C_J)\sin(\psi_e-\phi_e)}\mu^{1-\alpha} + \mathcal{O}(\mu^{2\alpha}), \\
\psi_s &= \psi_e + 4\mu^\alpha\frac{\cos(\psi_e-\phi_e)}{\sqrt{3-C_J}} \\
&\quad -\frac{2\cos(\psi_e-\phi_e)}{(3-C_J)\sin(\psi_e-\phi_e)}\mu^{1-\alpha} + \mathcal{O}(\mu^{2\alpha}), \\
v_s &= \sqrt{3-C_J-3\mu} + \frac{2\mu^{1-\alpha} + 3\cos^2\phi_s\mu^{2\alpha}}{2\sqrt{3-C_J}} + \mathcal{O}(\mu^{3\alpha}).
\end{aligned} \tag{45}$$

The expansions in (45) are in powers of μ^α and $\mu^{1-\alpha}$. We note that the lowest order congruence between these exponents, taking into account the restriction (3), is obtained for $2(1-\alpha) = 3\alpha$ and then $\alpha = 2/5$.

Let us consider now the case when $\psi_e - \phi_e = \pi + \Gamma\mu^\alpha$.

From (44) and (29),

$$\begin{aligned}
z_s &= -e^{i\phi_e/2}\frac{A+iB}{\sqrt{A^2+B^2}} + \mathcal{O}(\mu^\alpha), \\
w_s &= -e^{i\phi_e/2}\frac{C+iB}{\sqrt{A^2+B^2}} + \mathcal{O}(\mu^\alpha),
\end{aligned}$$

where

$$\begin{aligned}
A &= \frac{2\mu^{1-\alpha}}{3-C_J} + \mu^{2\alpha}\left(\frac{1+3\cos^2\phi_e}{3-C_J} - 2\left(\Gamma - \frac{1}{\sqrt{3-C_J}}\right)^2\right) + \mathcal{O}(\mu^{3\alpha}), \\
B &= 2\left(\Gamma - \frac{1}{\sqrt{3-C_J}}\right)\mu^\alpha + \frac{2\mu}{3-C_J}\left(2\Gamma - \frac{1}{\sqrt{3-C_J}}\right) + \mathcal{O}(\mu^{3\alpha}), \\
C &= \frac{2\mu^{1-\alpha}}{3-C_J} + \mu^{2\alpha}\frac{1+3\cos^2\phi_e}{3-C_J} + \mathcal{O}(\mu^{3\alpha}).
\end{aligned}$$

Setting $\Gamma = 1/\sqrt{3-C_J} + \eta\mu^{1-2\alpha}/(3-C_J)$, that is, $\psi_e - \phi_e = \pi + \mu^\alpha/\sqrt{3-C_J} + \eta\mu^{1-\alpha}/(3-C_J)$, we have

$$
\begin{aligned}
z_s &= -e^{i\phi_e/2}\frac{1+i\eta+\frac{1+3\cos^2\phi_e}{2}\mu^{3\alpha-1}+i\frac{\mu^\alpha}{\sqrt{3-C_J}}}{\sqrt{(1+\frac{1+3\cos^2\phi_e}{2}\mu^{3\alpha-1})^2+(\eta+\frac{\mu^\alpha}{\sqrt{3-C_J}})^2}}+\mathcal{O}(\mu^{4\alpha-1}),\\
w_s &= -e^{i\phi_e/2}\frac{1+i\eta+\frac{1+3\cos^2\phi_e}{2}\mu^{3\alpha-1}+i\frac{\mu^\alpha}{\sqrt{3-C_J}}}{\sqrt{(1+\frac{1+3\cos^2\phi_e}{2}\mu^{3\alpha-1})^2+(\eta+\frac{\mu^\alpha}{\sqrt{3-C_J}})^2}}+\mathcal{O}(\mu^{4\alpha-1}),
\end{aligned}
$$

and, going back through the changes (39), (36), (33) and (30), we obtain, close to collision,

$$
\begin{aligned}
\phi_s &= \phi_e+\Delta\phi-\frac{\eta(1+3\cos^2\phi_e)}{1+\eta^2}\mu^{3\alpha-1}-\frac{2\eta^2\mu^\alpha}{(1+\eta^2)\sqrt{3-C_J}}\\
&\quad+\frac{\eta(1+3\cos^2\phi_e)^2}{2(1+\eta^2)^2}\mu^{6\alpha-2}+\mathcal{O}(\mu^{4\alpha-1}),\\
\psi_s &= \phi_s+\Delta\phi-\frac{\mu^\alpha}{\sqrt{3-C_J}}+\mathcal{O}(\mu^{4\alpha-1}),
\end{aligned}
\tag{46}
$$

where

$$
\cos\Delta\phi=\frac{1-\eta^2}{1+\eta^2},\quad \sin\Delta\phi=\frac{2\eta}{1+\eta^2}.
$$

5. The return map on the resonant strips

In this section we shall always work in synodic coordinates, and the subscript s (resp. e) will mean as usual the configuration when the orbit is leaving (entering) the unit disk around the body M. Recall that, as seen in Section 2, for a certain value of the Jacobi constant C_J, a $p-q$ resonant strip is given in terms of the coordinates $(\phi,\xi)\in S^1\times[-\xi_m,\xi_m]\subset S^1\times(-1,1)$ by

$$
\psi_s=\tilde\psi_s-\mu^\alpha\frac{(B(\phi)+\xi C(\phi))}{\mathcal{K}}, \tag{47}
$$

where

$$
\begin{aligned}
v_0^2 &= 2-\left(\frac{p}{q}\right)^{2/3}\\
e &= \frac{(2-v_0^2)^{5/2}}{6\pi p},\\
\sin\tilde\psi_s &= \frac{4-C_J-v_0^2}{2\sqrt{3-C_J}},\\
\cos\tilde\psi_s &= \sigma\frac{\sqrt{4v_0^2-(2-C_J-v_0^2)^2}}{2\sqrt{3-C_J}},\\
B(\phi) &= \frac{1}{\sqrt{3-C_J}-\sin\tilde\psi_s}\left(2\cos\phi+\left(\sqrt{3-C_J}-\frac{e}{\cos\tilde\psi_s}\right)\sin(\phi-\tilde\psi_s)\right),\\
C(\phi) &= \frac{e}{(\sqrt{3-C_J}-\sin\tilde\psi_s)\cos\tilde\psi_s},\\
\mathcal{K} &= \frac{2(3-C_J)\cos\tilde\psi_s}{2-C_J+v_0^2},
\end{aligned}
\tag{48}
$$

and $\sigma = \text{sign }(\cos\tilde{\psi}_s)$. The condition $\xi_m < 1$ ensures that the resonant orbits enter the disk $\mathcal{D}$ away from tangency and so the hypothesis of Lemma 2.1 are fulfilled. From (28) and (47) the approximate expression for the OUT-map restricted to the $p-q$ resonant strip is given by

$$\phi_e = \tilde{\psi}_s + \pi - \arcsin\xi + \mathcal{O}(\mu^{1-2\alpha}),$$
$$\psi_e = \tilde{\psi}_s - \mu^\alpha\left((\epsilon' + \delta') + \frac{B(\phi) + \xi C(\phi)}{\mathcal{K}}\right) + \mathcal{O}(\mu^{1-\alpha}).$$

Using (26) and (48), the approximate OUT-map on the $p-q$ resonant strip becomes

$$\begin{aligned} \phi_e &= \tilde{\psi}_s + \pi - \arcsin\xi + \mathcal{O}(\mu^{1-2\alpha}), \\ \psi_e &= \tilde{\psi}_s - \mu^\alpha(k_1\cos\phi + k_2\sin\phi + k_3\xi + k_4\sqrt{1-\xi^2}) + \mathcal{O}(\mu^{1-\alpha}), \end{aligned} \tag{49}$$

with v_e given by (29) and

$$\begin{aligned} k_1 &= \frac{2e(4 - C_J - v_0^2)}{4v_0^2 - (2 - C_J - v_0^2)^2}, \\ k_2 &= -\frac{2\sigma e}{\sqrt{4v_0^2 - (2 - C_J - v_0^2)^2}}, \\ k_3 &= \frac{4e\sqrt{3 - C_J}}{4v_0^2 - (2 - C_J - v_0^2)^2} + \sigma\frac{2v_0^2 - 2}{\sqrt{3 - C_J}\sqrt{4v_0^2 - (2 - C_J - v_0^2)^2}}, \\ k_4 &= -\frac{2}{\sqrt{3 - C_J}}. \end{aligned}$$

Composing (49) and the first two equations in (45) we obtain the approximate expression for the global return map on the $p-q$ resonant strip far from collision, that is, when the modulus of ξ is much greater than the terms of order μ^α:

$$\begin{aligned} \phi_s &= \tilde{\psi}_s + \arcsin\xi + \mathcal{O}(\mu^{1-2\alpha}), \\ \psi_s &= \tilde{\psi}_s + \mu^\alpha g(\phi, \xi) + \mathcal{O}(\mu^{1-\alpha}), \end{aligned} \tag{50}$$

where

$$g(\phi, \xi) = -k_1\cos\phi - k_2\sin\phi - k_3\xi + k_4\sqrt{1-\xi^2}.$$

The behaviour of this return map is essentially the following: it maps each resonant strip on itself, after contracting by a factor of order $\mu^{1-2\alpha}$ along the horizontal direction, that is, the direction of the ϕ axis, and expanding by a factor of order $\mu^{-\alpha}$ along the vertical direction (the direction of the ψ axis). In fact, denoting by F the return map given by equations (50),we have

$$\left|\frac{\partial F}{\partial\phi}\right| = \mathcal{O}(\mu^{1-2\alpha}), \quad \left|\left(\frac{\partial F}{\partial\psi}\right)\right|^{-1} = \mathcal{O}(\mu^\alpha).$$

Notice that this hyperbolic behaviour is entirely due to the OUT-map. In fact, this analysis has been performed without taking into account the strongly hyperbolic behaviour of the IN-map when $\psi_e - \phi_e - \pi$ is of order μ^α . In order to check the behaviour of the IN-map for very small entrance angles we must compose (49) and, instead of (45), one should use (46) which applies when $\psi_e - \phi_e = \pi + \mu^\alpha/\sqrt{3 - C_J} + \eta\mu^{1-\alpha}/(3 - C_J)$. Then, taking now ϕ, η as coordinates on the resonant strip, the return map is

$$\begin{aligned} \phi_s &= \tilde{\psi}_s + \pi + \Delta\phi + \mathcal{O}(\mu^{3\alpha-1}) + \mathcal{O}(\mu^{1-2\alpha}), \\ \psi_s &= \tilde{\psi}_s + \pi + \Delta\phi + \mathcal{O}(\mu^{3\alpha-1}) + \mathcal{O}(\mu^{1-2\alpha}), \end{aligned} \tag{51}$$

where

$$\cos \Delta\phi = \frac{1-\eta^2}{1+\eta^2}, \quad \sin \Delta\phi = \frac{2\eta}{1+\eta^2}.$$

Instead of the second equation in (51), we may also use the second equation in (46) to obtain

$$\psi_s - \phi_s = -\frac{\mu^\alpha}{\sqrt{3-C_J}} + \mathcal{O}(\mu^{4\alpha-1}). \tag{52}$$

From equations (51) we see that the errors involved in the computation of the IN-map and of the OUT-map match for $\alpha = 2/5$. For this value of α, the error in the return map is of order $\mu^{1/5}$, and all the expansions are in integer powers of $\mu^{1/5}$. Equation (52) shows that the error in $\psi_s - \phi_s$ is smaller and of order $\mu^{3/5}$.

Close to collision approaches to M are mapped by the IN-map on ejections with arbitrary exit angle. The initial conditions on each resonant strip which correspond to these orbits lie on a small strip of width of order μ. The behaviour of the return map on this small strip is then as follows: horizontal contraction by a factor of order $\mu^{1/5}$, vertical expansion by a factor of order μ^{-1}, and the image lies along the $\phi = \psi$ line in (ϕ, ψ) space, thus intersecting transversally all the resonant strips except perhaps the initial (p, q)-resonant one.

Denoting now by F the global return map given by equations (50) and (51) in their regions of validity, we have that, for a given value of the Jacobi constant C_J, F is defined in the union of all the $p-q$ resonant strips for which (p, q) is admissible, that is, for which (19) holds, and that its qualitative behaviour is as shown in Figure 2. Then, by the well known properties of the horseshoe maps (see, for instance, [5]), we have the following

Theorem 5.1 *For any integer N, there exists $\mu(N)$ such that any admissible sequence (p_n, q_n) with $q_n < N$, $n \in \mathbb{Z}$, is realized by a consecutive quasi-collision orbit of the RTBP with $0 < \mu < \mu(N)$.*

Proof. What remains to be proved is that N is indeed arbitrary, since there are two constraints on N: on one hand, the period of the two body orbit with respect to E must be small enough for the error bounds of Section 2 to be valid, and on the other hand it must be small enough to prevent the existence of resonant strips μ^α close to each other.

Let us consider the first constraint. From equations (1), it is clear that the error done in the computation of the OUT-map when the body Z is not close to M is of order μ times p times the period of the two body orbit, or, which is the same, of order μ times q. Hence, $N\mu$ must be at most of order $\mu^{1-\alpha}$, that is, N must be much smaller than $1/\mu^\alpha$.

Consider now the second constraint. From equations (18), the distance between neighbouring resonant strips is of the order of the variation in the corresponding values of v_0^2, which, in turn, is of the order of the difference between the corresponding values of the quotient p/q. Therefore, $1/N$ must be much bigger than μ^α.

Hence, all the assumptions of the theorem hold provided that

$$\mu(N) \ll N^{-1/\alpha}. \tag{53}$$

6. Numerical results

In this section we shall first compare the perturbative results of the previous sections, namely the locus of the resonant strips and of their images under the OUT- and IN- maps with the corresponding numerical computations for small values of the parameter μ. Also for small values of μ, we shall present some numerical examples of periodic orbits of this problem which visit small neighbourhoods of the primary M. Finally, we shall examine the changes as μ increases and new phenomena appear.

All the orbits are obtained by numerical integration of the equations of the RTBP with regularization of collision with the small primary M, using the Runge-Kutta-Fehlberg algorithms of orders 7-8.

We take the parameter $\alpha = 2/5$ since the errors involved in the analytic computations of the OUT- and the IN- maps match for this value of α, and the global error estimate for the return map is then of order $\mu^{1/5}$.

The numerical procedure to find a $p - q$ resonant strip is the following:

(i) We fix a value for μ, C_J and the index $\sigma = \pm 1$ of the strip.

(ii) We take an initial condition leaving the disk $\mathcal{D}$, defined by a pair ϕ, ψ. Note that since p, q and σ are fixed, ψ must be close to $\tilde{\psi}_s$ defined by (18).

(iii) Keeping ϕ fixed, we change ψ in a neighbourhood of $\tilde{\psi}_s$ until we find a value for which the orbit, after approximately $2\pi q$ time units, has a tangency with the circle $\partial\mathcal{D}$. Thus we have found an initial condition in the ϕ, ψ torus which belongs to the boundary of the (p, q, σ) resonant strip (say point P in Figure 2.a)).

(iv) We increase ϕ using a continuation method to keep ψ on the boundary a of the strip until we reach the line $\phi = \psi + \pi/2$ (point B in Figure 2.a)).

(v) On the line $\phi = \psi + \pi/2$ (line b in Figure 2.a)), we look for another initial condition which will also give rise to a tangency with $\partial\mathcal{D}$ (point C in Figure 2.a)). Note that, since the $p - q$ resonant strip is by definition the locus of the initial conditions on the ϕ, ψ torus whose orbits meet again the disk $\mathcal{D}$ after approximately $2\pi q$ time units, it is bounded by two lines which correspond to two different tangencies with $\partial\mathcal{D}$, on both sides of M. This is represented in Figure 2.b).

(vi) We decrease ϕ using a continuation method to keep ψ on the boundary c until we reach the line $\phi = \psi - \pi/2$ (point D in Figure 2.a)).

(vii) On the line $\phi = \psi - \pi/2$ (line d in Figure 2.a)) we look for point A as in 5.

(viii) We increase ϕ using again a continuation method until we reach point P.

In Figure 3, as well as in all the subsequent figures representing resonant strips and their images, ϕ and ψ are the coordinates along the horizontal and vertical axis,

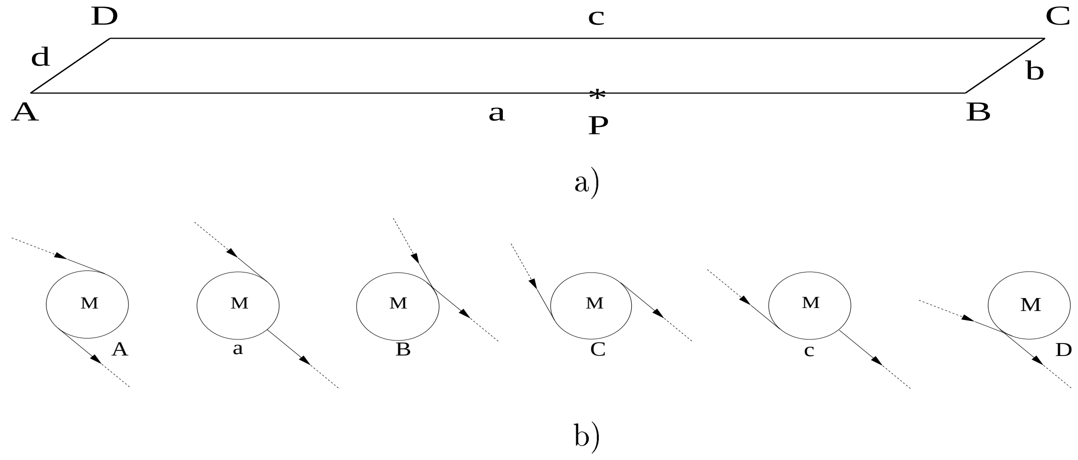

Figure 2. a) The boundary of a resonant strip. b) Qualitative changes as we proceed along the boundary.

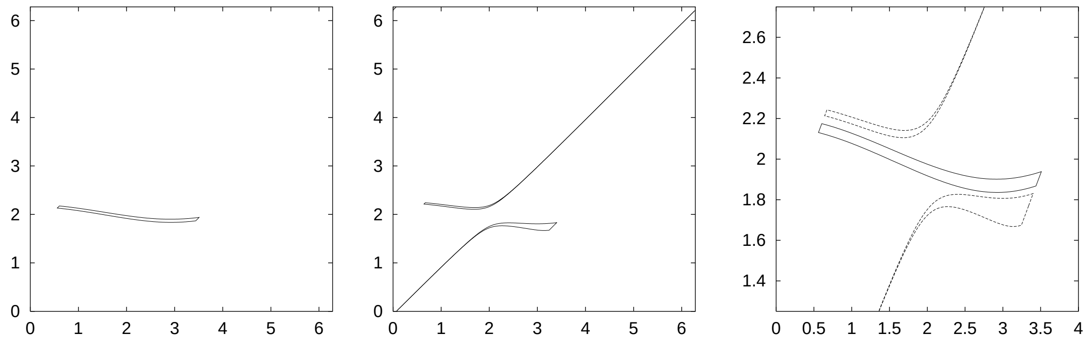

Figure 3. For $C_J = 2.8$ and $\mu = 10^{-4}$, the $(p = 2, q = 1, \sigma = -1)$ resonant strip, its image and an enlargement of the resonant strip together with its image. In this and subsequent figures representing resonant strips and their images, ϕ and ψ are the coordinates along the horizontal and vertical axis, respectively.

respectively. In Figure 3 we have taken $C_J = 2.8$ and $\mu = 10^{-4}$, and we have plotted the $(p = 1, q = 2, \sigma = -1)$ resonant strip and its image, obtained by integrating the orbits with initial conditions on the boundary of the resonant strip until their second intersection with $\partial\mathcal{D}$. Due to the high stretching rate of the map, it is necessary to take a small step size on the lines that correspond to lines b and d of Figure 2.a). In fact, it is convenient to take a non uniform step size on these lines, decreasing as we come closer to collision. In the last plot of Figure 3 we have plotted both the strip and its image and we have rescaled around the resonant strip.

In Figure 4 we show a similar plot for the $(p = 5, q = 3, \sigma = -1)$ resonant strip and its image as μ takes the values 10^{-6}, 10^{-4} and 10^{-3}.

For $C_J = 2.8$ (the results for other values of the Jacobi constant are similar) we have computed the admissible (p, q) pairs with $q \leq 7$ using (19). We took this bound on q because of the restriction $q << \mu^{-\alpha}$ (see 53) and of the fact that we want to consider values of μ as high as 10^{-3}. Note that for this value of μ the bound $N = 7$ is not even

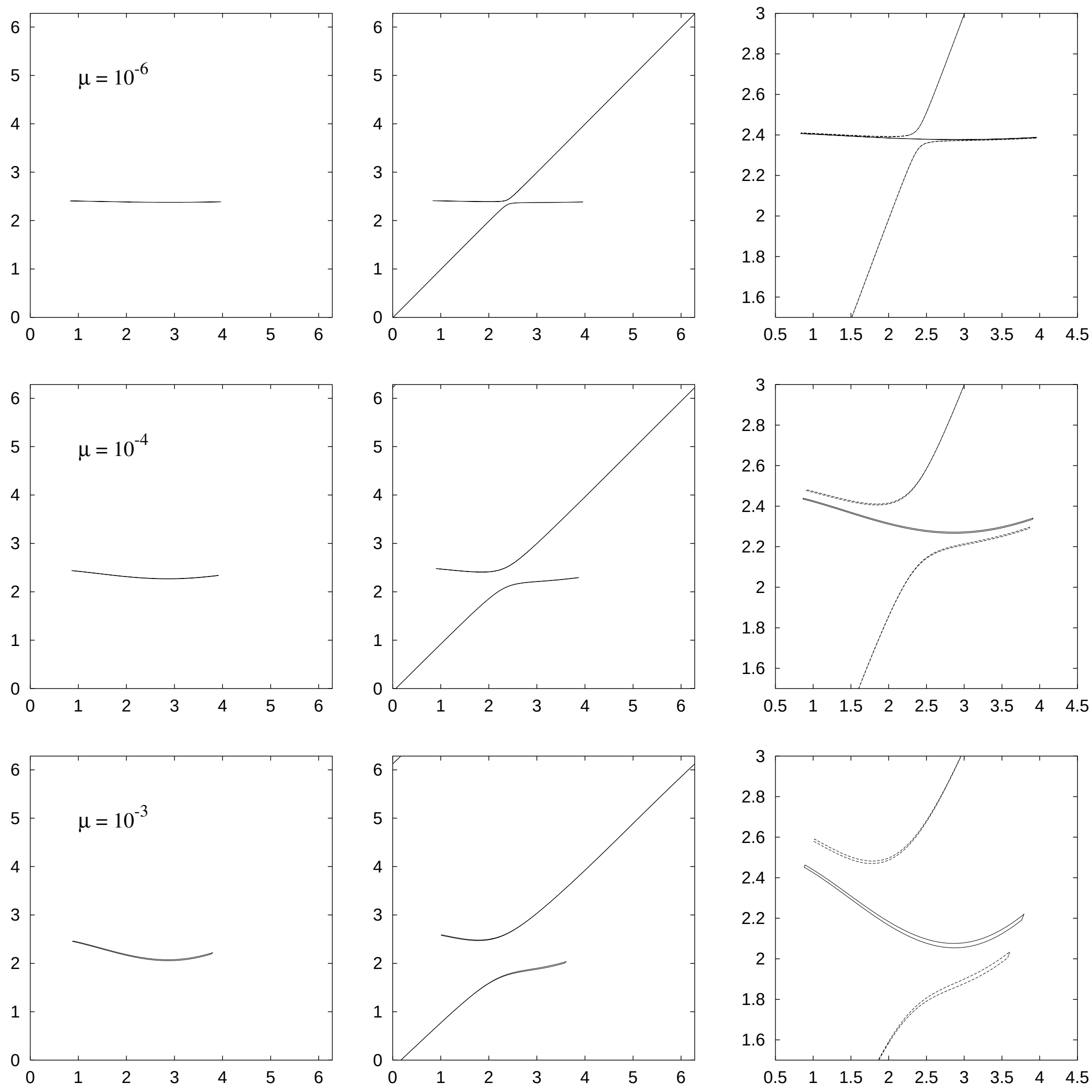

Figure 4. For $C_J = 2.8$, the $(p = 5, q = 3, \sigma = -1)$ resonant strip, its image, and the resonant strip together with its image. From top to bottom, μ takes the values 10^{-6}, 10^{-4} and 10^{-3}.

small compared to $\mu^{-2/5}$. From the list of admissible (p, q) pairs for $C_J = 2.8$ given by (19) we must remove those which correspond to orbits that involve intermediate close encounters between the body Z and M, that is, close encounters between these two bodies apart from the resonances we consider. By a close encounter it is meant, in accordance with the hypothesis of Lemma 2.1, that the distance between Z and M becomes of order $\mu^{\alpha/2}$. To determine the pairs (p, q) which give rise to intermediate close encounters we have used an algorithm based on Hénon's work [2], and we have taken $\mu = 10^{-3}$. An intermediate close encounter is associated with a crossing point $\mathcal{P}$ of the sidereal two-body orbits of Z and M around E such that the passage of Z and M through $\mathcal{P}$ takes place away from resonance and the time interval Δt between the passage of Z and that of M through $\mathcal{P}$ is small. We have computed the pairs (p, q) for

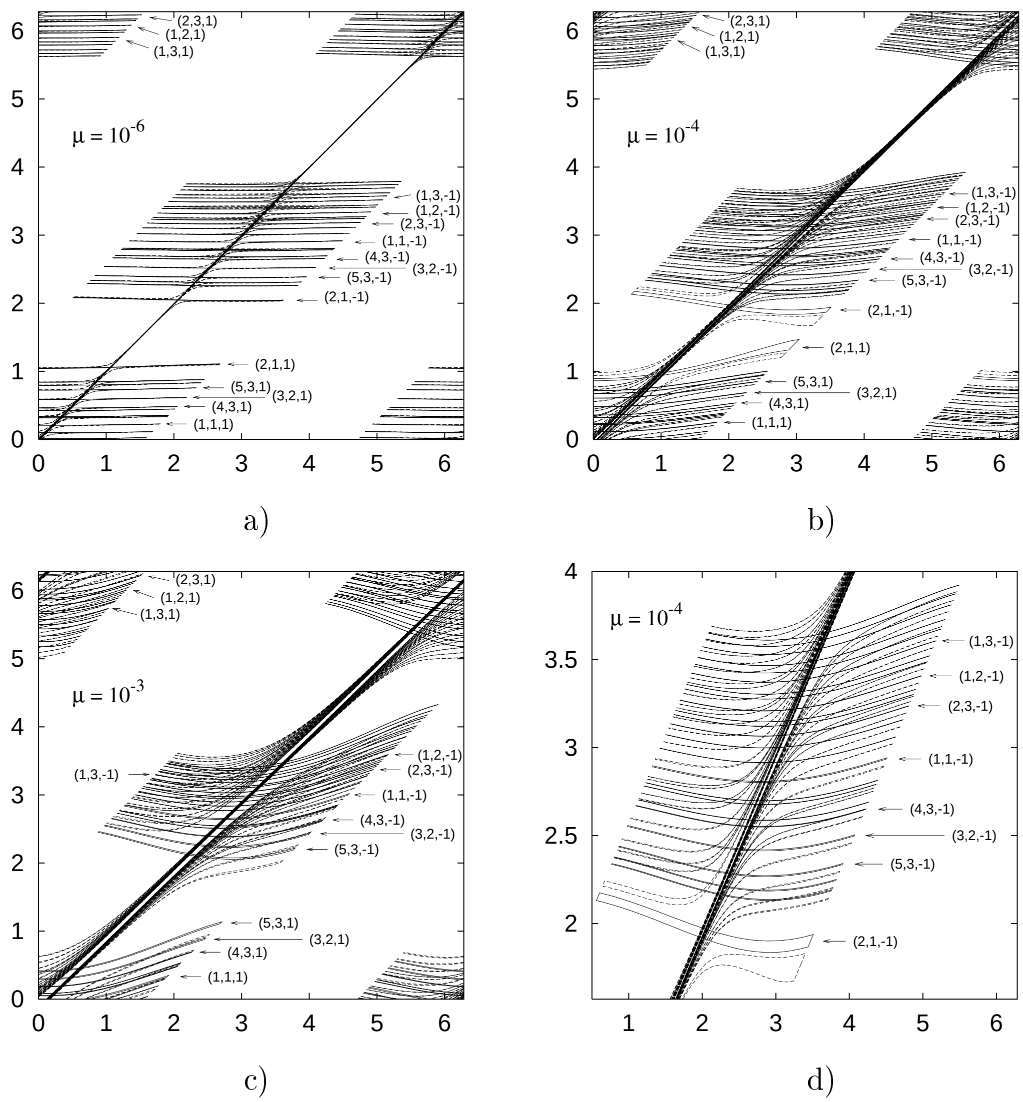

Figure 5. For $C_J = 2.8$, the set of admissible resonant strips up to $q = 7$ (plotted with lines) and the corresponding images (plotted with dotted lines), as μ takes the values (a) $\mu = 10^{-6}$, (b) $\mu = 10^{-4}$ and (c) $\mu = 10^{-3}$. The resonant strips for which $q \leq 3$ have been labeled. d) Partial and enlarged plot of b).

which this Δt is smaller than $(10^{-3})^{1/5}$ and found the set of pairs

$$\begin{array}{l}\{(5,4),(4,5),(6,5),(7,5),(8,5),(11,5),(5,6),(11,6),(13,6),\\ \quad (5,7),(10,7),(11,7),(12,7),(13,7),(15,7)\}\end{array} \tag{54}$$

which are excluded from the set of admissible values.

In Figure 5 we have plotted the numerical resonant strips and their images for each of the remaining (p, q, σ) values and for $\mu = 10^{-6}$ (Figure 5.a)), $\mu = 10^{-4}$ (Figure 5.b) and, enlarged, Figure 5.d)) and $\mu = 10^{-3}$ (Figure 5.c)).

For the plots in Figure 6.a) we have taken $C_J = 1.8$ and we have considered in detail the $(p = 3, q = 2, \sigma = 1)$ resonant strip for, from top to bottom, $\mu = 10^{-6}$, $\mu = 10^{-4}$ and $\mu = 10^{-3}$. Each plot includes the numerical resonant strip and its image as well

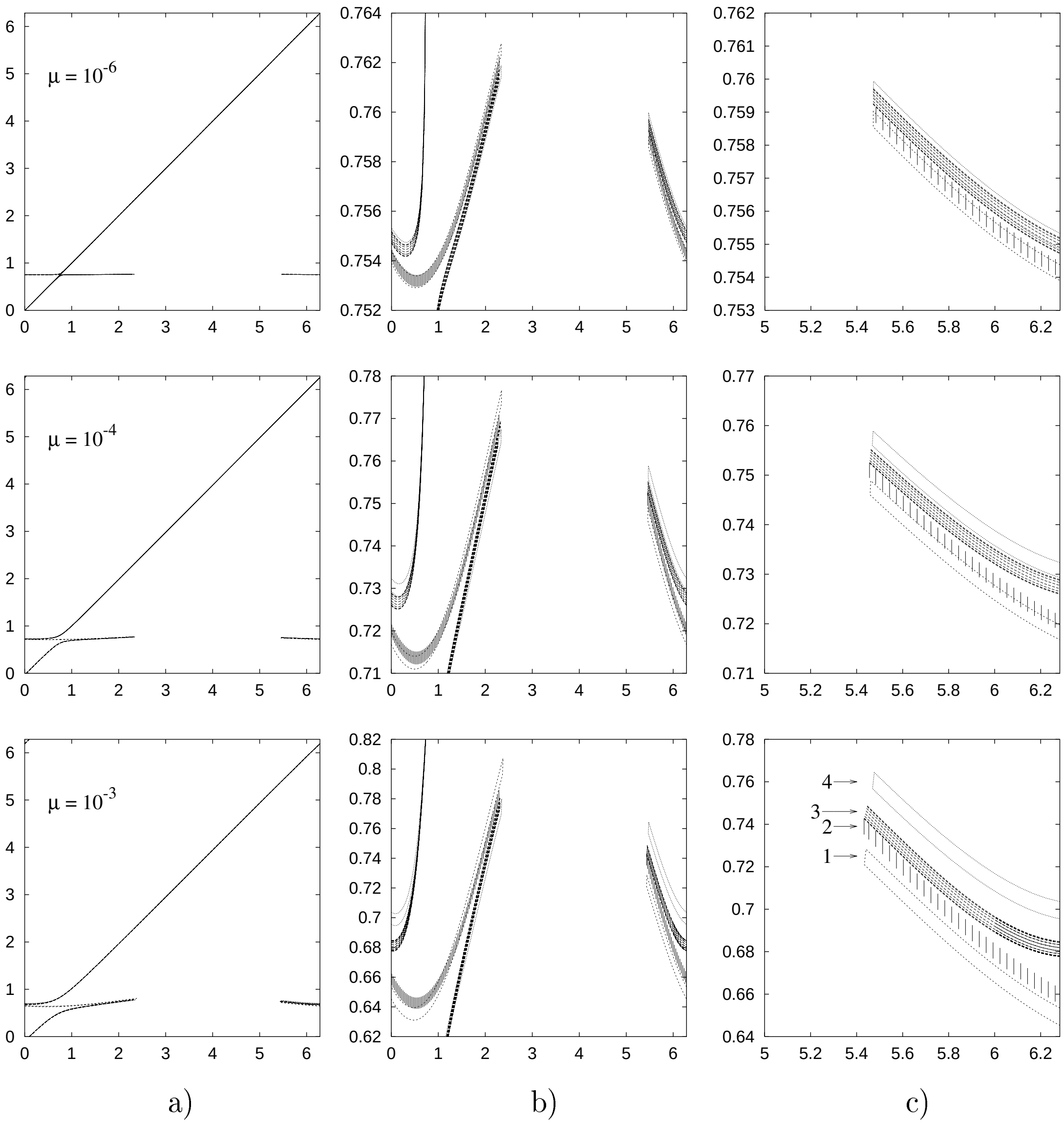

Figure 6. a) For $C_J = 1.8$ and $(p = 3, q = 2, \sigma = 1)$, the numerical resonant strip and its image, and the analytic resonant strip and its image by the approximate return map. From top to bottom, $\mu = 10^{-6}$, $\mu = 10^{-4}$ and $\mu = 10^{-3}$. The columns b) and c) display enlargements of column a) around the resonant strip. The numerical resonant strip (1) is plotted with a dotted line, its image (4) with a broken line, the analytic resonant strip (2) is filled with vertical segments, and its image (3) by the approximate return map is the shadowed strip.

as the analytic resonant strip (given by 47) and its image by the approximate return map (given by equations 49 and 44). This is shown with increasing detail in Figures 6.b) and 6.c), where it can be seen that numerical curves are well approximated by the analytical curves, even for $\mu = 10^{-3}$. In column c) it can be seen that, for the analytical approximations, the resonant strips and their images are very close near the left end. In the numerical plots they are well separated, but this separation has been checked to be $O(\mu^{\gamma}), \gamma \geq 2/3$, and hence of the order of the error terms of the analytical expressions.

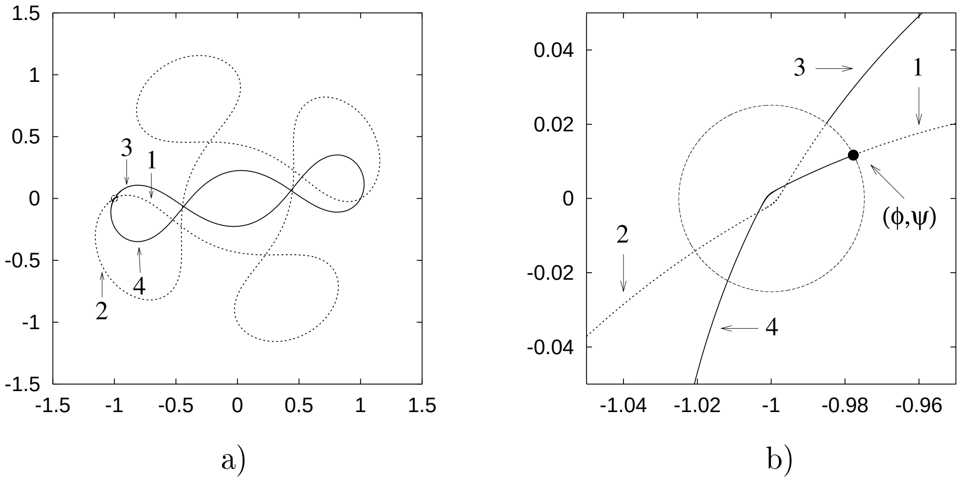

Figure 7. a) A POSS periodic orbit for $C_J = 2.8$, $\mu = 10^{-4}$. The horizontal and vertical axis are the synodic x and y axis, respectively. The initial conditions are $(\phi, \psi) \simeq (0.4840458051695259, 0.3657582929540782)$, the orbit is unstable and the stability parameter is near to 2.338645E+7. As time increases, the orbit goes through the arcs 1, 2, 3 and 4. The dotted line, from 1 to 2, is the part of the orbit associated with the $(p = 4, q = 3, \sigma = 1)$ resonance, and the full line, from 3 to 4, is the part of the orbit associated with the $(p = 2, q = 1, \sigma = 1)$ resonance. b) The behaviour of the orbit as it goes through the ball of radius μ^{α}.

As predicted by Theorem 5.1, there exist infinitely many unstable periodic orbits associated to periodic sequences $(p_n, q_n, \sigma_n)_{n\in\mathbb{Z}}$. We use extended precision to compute the periodic orbits and the stability parameter. In Figure 7 and for $\mu = 10^{-4}$, $C_J = 2.8$ we show one of these orbits for which $(p_n, q_n, \sigma_n) = (4, 3, +1)$ if n odd and $(2, 1, +1)$ for n even. For the same values of μ and C_J and the sequences $(2, 1, +1)$ for n odd, $(2, 1, -1)$ for n even a periodic orbit is displayed in Figure 8. The existence of these orbits was first conjectured by Poincaré ([7]), who called them periodic orbits of the second species (POSS). We remark that the orbit shown in Figure 7 is not symmetric with respect to the synodic x-axis and in Figure 8 we show a symmetric orbit with respect to the synodic x-axis. Most of the periodic orbits given by Theorem 5.1 are asymmetric, but it is possible to obtain symmetric periodic orbits, for instance, by taking a sequence of the form (p, q, σ) if n odd and $(p, q, -\sigma)$ if n even.

Another example of an asymmetric POSS is shown in Figure 9. Here, the corresponding symbolic sequence $(p_n, q_n, \sigma_n)_{n\in\mathbb{Z}}$ is the period three sequence formed by the triplets $(2, 1, 1)$, $(2, 1, -1)$, $(3, 2, 1)$.

Going back now to Figure 5, we see that, as the parameter μ increases from 10^{-4} to 10^{-3}, several resonant strips have been lost. This may be due to two different causes.

One of them is illustrated by the disappearance of the $(9, 7, \pm 1)$ strips. Although $(9, 7)$ is not in the set (54), if we define a close encounter in a slightly less restrictive way, say by requiring Δt to be smaller than $1.6 \times (10^{-3})^{1/5}$, we find that the corresponding orbit has two close encounters between resonances. The resulting

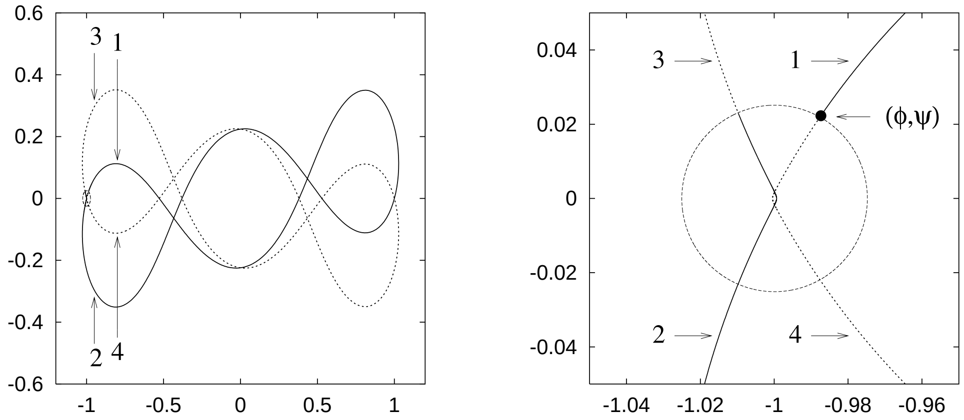

a) b)

Figure 8. a) A symmetric POSS periodic orbit for $C_J = 2.8$, $\mu = 10^{-4}$. The horizontal and vertical axis are the synodic x and y axis, respectively. The initial conditions are $(\phi, \psi) \simeq (1.060031115468069, 0.9672594502381595)$, the orbit is unstable and the stability parameter is near to 1.132360E+6. As time increases, the orbit goes through the arcs 1, 2, 3 and 4. The dotted line, from 1 to 2, is the part of the orbit associated with the $(p = 2, q = 1, \sigma = 1)$ resonance, and the full line, from 3 to 4, is the part of the orbit associated with the $(p = 2, q = 1, \sigma = -1)$ resonance. b) The behaviour of the orbit as it goes through the ball of radius μ^{α}.

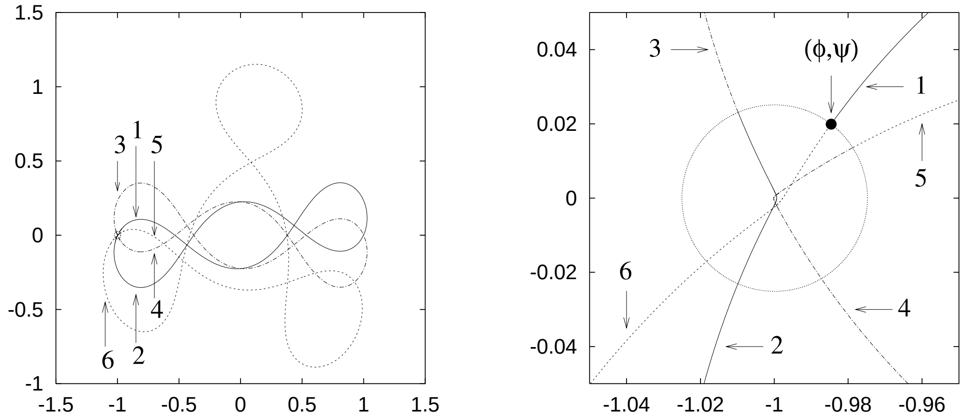

a) b)

Figure 9. a) A POSS periodic orbit for $C_J = 2.8$, $\mu = 10^{-4}$. The horizontal and vertical axis are the synodic x and y axis, respectively. The initial conditions are $(\phi, \psi) \simeq (0.91622091785178612688, 0.94492534193201301129)$ the orbit is unstable and the stability parameter is near to -4.228471E+9. As time increases, the orbit goes through the arcs 1, 2, 3, 4, 5 and 6. The full line, from 1 to 2, is the part of the orbit associated with the $(p = 2, q = 1, \sigma = 1)$ resonance, the dashed line, from 3 to 4, is the part of the orbit associated with the $(p = 2, q = 1, \sigma = -1)$ resonance, and the dotted line, from 5 to 6, is the part of the orbit associated with the $(p = 3, q = 2, \sigma = 1)$ resonance. b) The behaviour of the orbit as it goes through the ball of radius μ^{α}.

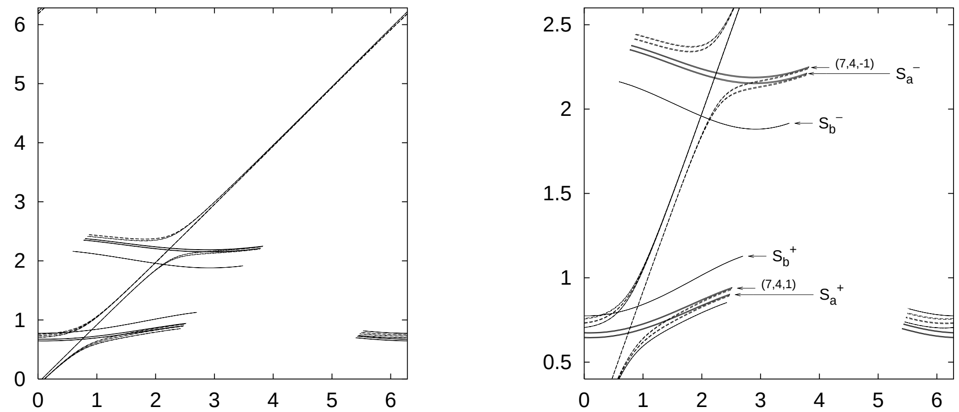

a) b)

Figure 10. The resonant strips (7,4,+1) and (7,4,-1) and the sets S_a^+, S_a^-, S_b^+ and S_b^- together with their images for $\mu = 10^{-4}$. a) $(\phi, \psi) \in [0, 2\pi] \times [0, 2\pi]$. b) $(\phi, \psi) \in [0, 2\pi] \times [0.4, 2.6]$.

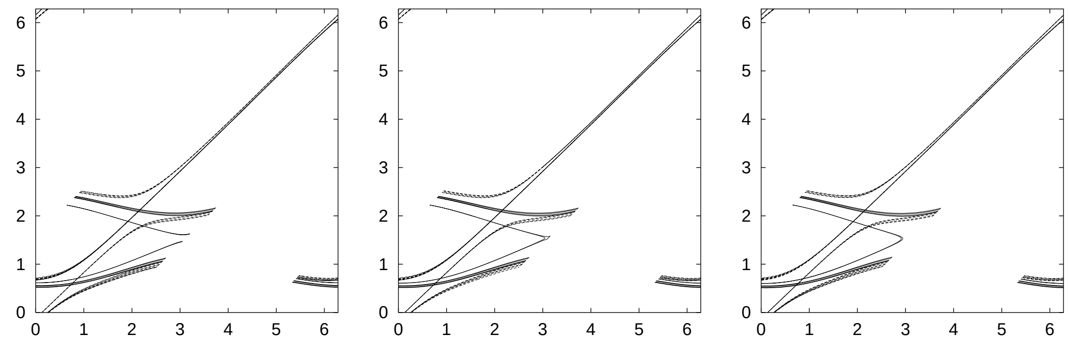

a) b) c)

Figure 11. The resonant strips (7,4,+1) and (7,4,-1) and the sets $S_{a,b}^{+,-}$, together with their images, for several values of μ. a) $\mu = 5 \times 10^{-4}$, b) $\mu = 5.25 \times 10^{-4}$, c) $\mu = 5.5 \times 10^{-4}$. Here, S_b^- and S_b^+ have merged to form the connected set S.

accumulated perturbation destroys the resonant strip.

The other mechanism is more subtle. In this case, the resonant orbits still exist, but the locus of the corresponding initial conditions is strongly deformed. It ceases to be close to a horizontal strip, the analytical theory cannot be applied (μ is too large) and it can no longer be found by our standard numerical procedure. To illustrate this phenomenon, we have followed in detail the behaviour of the $(7, 4, +1)$ strip, one of the missing strips in Figure 5.c), as μ increases from 10^{-4} to 1.5×10^{-3}.

In Figure 10 we have plotted, together with their images, the boundaries of the $(7, 4, +1)$ and $(7, 4, -1)$ strips for $\mu = 10^{-4}$. We have also plotted in this figure, together with their images, the boundaries of four other connected sets of initial conditions of orbits that return to the disk $\mathcal{D}$ after approximately $2\pi q$ time units. These sets, that we

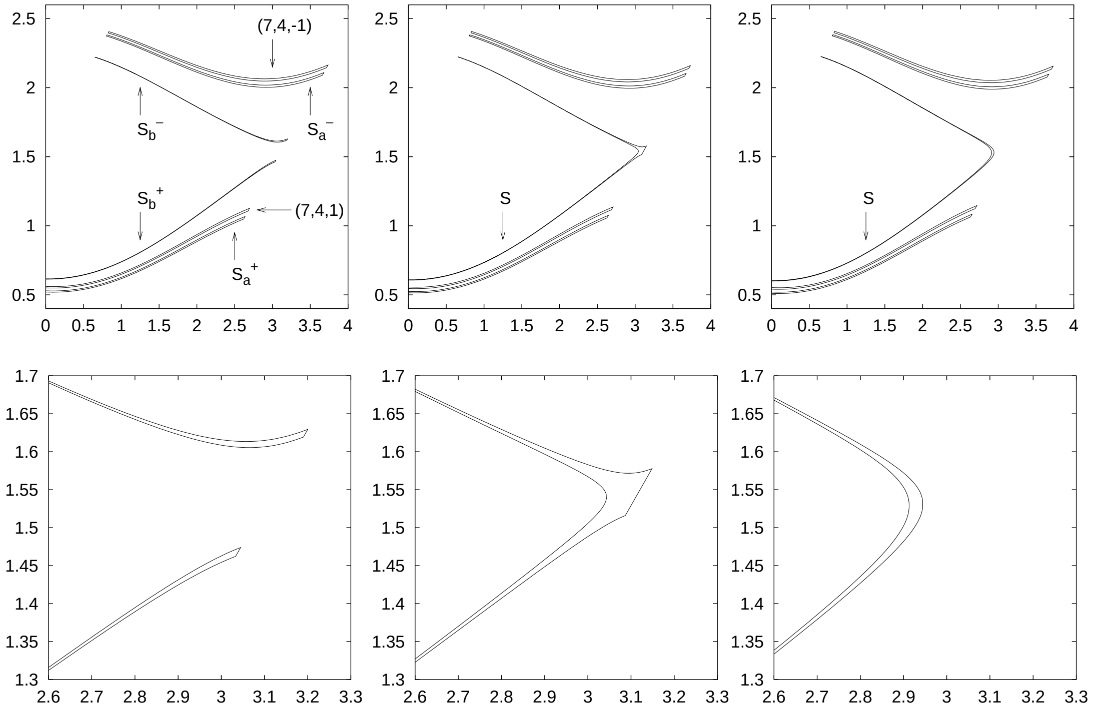

a) b) c)

Figure 12. The resonant strips (7,4,+1) and (7,4,-1) and the sets $S^{+;-}_{a,b}$ are shown here in a different scale ($(\phi,\psi)\in[0,4]\times[0.4,2.6]$, top figures, and $(\phi,\psi)\in[2.6,3.3]\times[1.3,1.7]$, bottom figures) for the same values of μ as in Figure 11. In the bottom figures we may see in more detail how the sets S^-_b and S^+_b have merged for $\mu = 5.5\times10^{-4}$ to form the connected set S. The merging takes place for ψ close to $\pi/2$. a) $\mu = 5\times10^{-4}$, b) $\mu = 5.25\times10^{-4}$, c) $\mu = 5.5\times10^{-4}$.

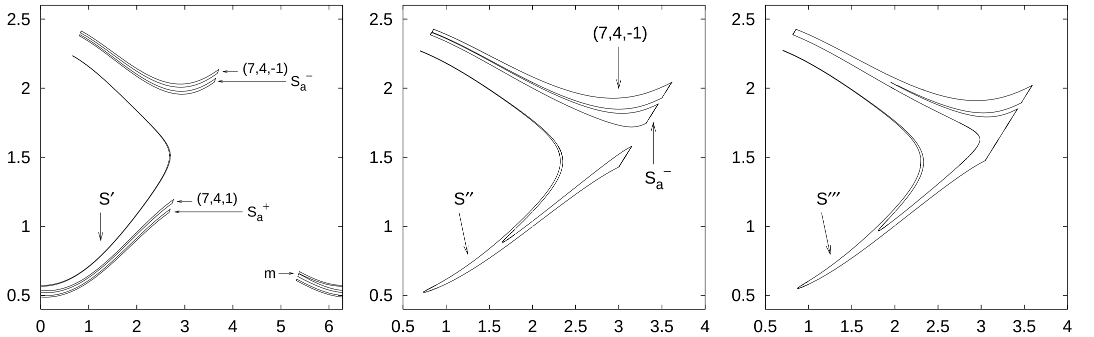

a) b) c)

Figure 13. The resonant strips (7,4,+1) and (7,4,-1) and the sets S, S^+_a, and S^-_a are shown here in different scales for bigger values of μ. a) $\mu = 6.74\times10^{-4}$, ($(\phi,\psi)\in[0,2\pi]\times[0.4,2.6]$). The set S and the resonant strip (7,4,+1) have merged to form the set S' (the merging taking place at the place labeled m). b) $\mu = 1.4\times10^{-3}$, ($(\phi,\psi)\in[0.5,4]\times[0.4,2.6]$). S' and S^+_a have merged to give $S''$and the resonant strip (7,4,-1) and the set S^-_a are close to each other. c) $\mu = 1.5\times10^{-3}$, ($(\phi,\psi)\in[0.5,4]\times[0.4,2.6]$). S'', (7,4,-1) and S^-_a merged to form a unique connected set S'''.

shall call S_a^+, S_a^-, S_b^+ and S_b^-, are not $(7,4)$ resonant strips, and they appear close to the $(7,4,+1)$ (S_a^+ and S_b^+) and $(7,4,-1)$ (S_a^- and S_b^-) strips as μ increases and we allow a bigger error in the return time. All the initial conditions on the sets $S_{a,b}^{+,-}$ involve intermediate close encounters or correspond to return times which differ significantly (about 5%) from $2\pi q$. These sets play a crucial role in the death of the resonant strips. This can be seen in more detail in the following figures.

In Figures 11 and 12 we may see how the sets S_b^- and S_b^+ merge for μ around 5.25×10^{-4} to form a unique connected component S. This set S will in turn merge with the $(7,4,+1)$ strip for μ around 6.74×10^{-4}, as shown in Figure 13.a), to form the set S'. As μ increases, the ϕ range of the set S' gets smaller and S' merges with the set S_a^+, producing a connected set S'', for μ around 1.4×10^{-3}, while (7,4,-1) and S_a^- get closer (see Figure 13.b)). For μ still bigger, these three sets merge to form a unique connected set S'''(see Figure 13.c)).

7. Conclusions

The existence of orbits having consecutive passages very close to the smallest of the primaries (quasi-collisions) in the RTBP has been shown. Furthermore the passages can be selected with some “randomness” due to the freedom in selecting the involved resonances between the mean motions. Concerning this problem existence results are available in the literature, but we have taken a direct and more constructive approach which allows to make accurate predictions of the initial conditions. This is illustrated with some highly unstable periodic orbits, either symmetric or not.

For conciseness we have considered the case when the quasi-collisions take place, essentially, around the same location in sidereal coordinates. The same ideas can be used when quasi-collisions taking place inear different locations along the orbit of the smallest primary, occur.

Beyond theoretical considerations these orbits are relevant when it is interesting to perform successive fly-byes of the small primary by a spacecraft. This can help to put the spacecraft on a desireal nominal orbit around the largest primary at low cost.

Acknowledgments

The work of second author (A.N.) has been partially supported by an EEC HCMP Grant no. ERBCHBICT941000. The work of the first and third authors has been supported by CIRIT Grant 1998 S0GR-42 (Catalonia) and DGICYT PB94-215 (Spain).

References

[1] BOLOTIN S V and MACKAY R S 2000 Periodic and chaotic trajectories of the second species for the $n-$centre problem To appear in *Celestial Mechanics*

[2] HÉNON M 1966 Sur les Orbites Interplanétaires qui Rencontrent Deux Foix la Terre *Bulletin Astronomique de Paris* **1** 377–402

[3] HENRARD J 1980 On Poincaré's Second Species Solutions *Celestial Mechanics* **25** 83–97

[4] MARCO J P and NIEDERMAN L 1995 Sur la construction des solutions de seconde espèce dans le problème plan restrient des trois corps *Ann. Inst. H. Poincaré Phys. Théor.* **62** 211–249

[5] MOSER J 1973 *Stable and Random Motions in Dynamical Systems* Princeton University Press, Princeton

[6] PERKO L 1976 Second Species Periodic Solutions with an $\mathcal{O}(\mu)$ Near-Moon Passage *Celestial Mechanics* **14** 395–427

[7] POINCARÉ H 1899 *Les Méthodes Nouvelles de la Mécanique Celeste. Tome III* Gauthier-Villars

[8] SZEBEHELY V 1967 *Theory of Orbits* Academic Press, New York